



**NEAR EAST UNIVERSITY
INSTITUTE OF GRADUATE STUDIES
DEPARTMENT OF CIVIL ENGINEERING**

**DEVELOPING AN ASPHALT PAVEMENT CRACK DETECTION
AND CLASSIFICATION MODEL BY USING BEAMLET
TRANSFORM ALGORITHM**

M.Sc. THESIS

Hassan Idow MOHAMED

Nicosia

October, 2023

HASSAN IDOW MOAHMED

**DEVELOPING AN ASPHALT PAVEMENT CRACK
DETECTION AND CLASSIFICATION MODEL BY USING
BEAMLET TRANSFORM ALGORITHM**

**NEU
2023**

**NEAR EAST UNIVERSITY
INSTITUTE OF GRADUATE STUDIES
DEPARTMENT OF CIVIL ENGINEERING**

**DEVELOPING AN ASPHALT PAVEMENT CRACK DETECTION AND
CLASSIFICATION MODEL BY USING BEAMLET TRANSFORM
ALGORITHM**

M.Sc. THESIS

Hassan Idow MOHAMED

Supervisor




Assist. Prof. Dr. Mustafa ALAS

Nicosia

October, 2023

Approval

We certify that we have read the thesis submitted by **Hassan Idow MOHAMED** titled “**DEVELOPING AN ASPHALT PAVEMENT CRACK DETECTION AND CLASSIFICATION MODEL BY USING BEAMLET TRANSFORM ALGORITHM**” and that in our combined opinion it is fully adequate, in scope and in quality, as a thesis for the degree of Master of Educational Sciences.

Examining Committee	Name-Surname	Signature
Head of the Committee:	Assoc. Prof. Dr. Shaban Ismael Albrka 
Committee Member:	Assoc. Prof. Dr. Hussin A.M Yahia 
Supervisor:	Assist. Prof. Dr. Mustafa ALAS 

Approved by the Head of the Department

.20./10../2023



Prof. Dr. Kabir Sadeghi

Head of Civil Engineering Department.

Approved by the Institute of Graduate Studies

...../...../2023

Prof. Dr. Kemal Hüsni Can Başer

Head of the Institute of Graduate Studies.



Declaration

I hereby declare that all information, documents, analysis and results in this thesis have been collected and presented according to the academic rules and ethical guidelines of the institute of graduate studies, Near East University. I also declare that as required by these rules and conduct, I have fully cited and referenced information and data that are not original to this study.

A handwritten signature in black ink, appearing to read 'HASSAN IDOW MOHAMED', with a long horizontal line extending to the left.

Hassan Idow MOHAMED

10 /16/2023

Acknowledgments

First of all, we are very grateful to Allah the Almighty for giving us the Strength and the courage to complete this thesis. also, I want to thank our parents for their prayers and encouragement. Several people who have been a backbone to complete and without their help and guidance that this thesis would have not been completed. I would like to express our deepest gratitude for helping us during our years as engineering students.

Assist. Prof. Dr. Mustafa ALAS, my advisor has been guiding us through every step of this thesis; he has overseen the progress of thesis, modeling, and proper implementation of design codes. In addition, he was literally making sure that I am on the right track from the very beginning to the very end of the thesis. Thank you for giving us the delight of working as engineers, and being patient for supporting us to achieve the thesis. Thank you for your time and effort.

I want to thank my appreciation to all of the professors and instructors at Near East University for spreading knowledge and offering sincere and valuable support during the course.

Also, I want to thank everyone who had a hand in providing us with what I needed to complete the work from outside the university in different domains, and of course, our families who stood by us all the time and applied all the effort to help us reach where I am now.

Abstract**DEVELOPING AN ASPHALT PAVEMENT CRACK DETECTION AND CLASSIFICATION MODEL BY USING BEAMLET TRANSFORM ALGORITHM.****Hassan Idow MOHAMED, Assist. Prof. Dr. Mustafa ALAS****MSc, Department of Civil Engineering, Faculty of Civil and Environmental Engineering, Near East University, Nicosia.****October, 2023, 77 Pages**

Pavement cracking is a common road infrastructure issue which significantly affects road performance, safety and longevity. This thesis employed a Beamlet Transform algorithm to detect and classify different types of flexible asphalt concrete pavement cracks. Additionally, a dedicated crack segmentation network was employed for precise segmentation of pavement crack. This approach incorporates advancements that has improve precision in crack classification and segmentation. Based on the results of the beamlet transform, significant improvements in the gray scale representation of crack, enhanced crack detection, reduced noise in crack images and a more precise measurement of cracks length were achieved. Computations were performed to determine the length of linear cracks and the area of block cracks. A total of 1000 pavement images were used for training and testing the accuracy of asphalt pavement crack detection and classification models. The research results showed that block cracking, alligator cracking, transverse cracking, and longitudinal cracking can all be recognized with a remarkable accuracy. Alligator cracks and block cracks achieved detection rates more than 90%, while detection rates for the longitudinal and transverse cracks reached more than 95% accuracy.

Keywords: Pavement crack detection, Crack classification, Longitudinal crack, Alligator crack, Block crack, Transverse crack, Beamlet transform.

Table of Contents

Approval.....	i
Declaration	ii
Acknowledgments	iii
Abstract	iv
Table of Contents.....	v
List of Figures.....	viii
List of Tables.....	ix
List of Abbreviations	x
CHAPTER I	1
Introduction	1
1.1 Background.....	1
1.2 Aim of the Study.....	2
1.3 Objectives of the Study	2
1.4 Problem Statement	2
1.5 Research Question.....	3
1.6 Scope of the Study	3
1.7 Limitations.....	3
CHAPTER II	4
Literature Review	4
2.1 Introduction	4
2.1 Background in digital image processing	4
2.1 Cracking phenomenon understanding.....	6
2.3 Crack classification based on types of cracks	9
2.3.1 Fatigue cracks	9
2.3.2 Block cracks.....	10
2.3.3 Edge cracks.....	10
2.3.4 Longitudinal cracks	11
2.3.5 Reflection cracks.....	12
2.3.6 Transverse cracks	12
2.4 Crack processing using traditional digital image processing	13
2.4.1 Edge detection.....	14

2.4.2 Gabor filters	17
2.4.3 Adaptive thresholding	18
2.4.4 Crack detection based on image features	19
2.4.5 Geography features	20
2.5 Background in machine learning	22
2.5.1 Crack processing based on machine learning with convolutional neural networks	22
2.5.2 Crack detection	22
2.5.3 Crack segmentation	25
CHAPTER III	29
Methodology	29
3.1 Overview	29
3.2 Crack classification standard	29
3.3 Method	30
3.3.1 Beamlet transform algorithm image processing	30
3.4 Beamlet algorithm	31
3.4.1 Beamlet dictionary	31
3.4.2 Beamlet transform	32
3.4.3 Algorithm flow	34
CHAPTER IV	35
Result and Discussion	35
CHAPTER V	55
Conclusion	55
Recommendation	55
References	57
Appendix	72
Appendix A MATLAB code	73
Appendix B Ethics Certificate	76
Appendix C Turnitin Similarity Report	77

List of Figures

Figure 2.1 Crack analysis on road images.	7
Figure 2.2 Fatigue crack examples.	9
Figure 2.3 Block cracks.....	10
Figure 2.4 Edge cracks.....	11
Figure 2.5 Longitudinal cracks.....	11
Figure 2.6 Reflection cracks.....	12
Figure 2.7 Transverse cracks.....	13
Figure 2.8 Improved canny method result.	14
Figure 2.9 Edge detection experimentation results for pavement image.....	16
Figure 2.10 Gabor filter applied to a road image.	17
Figure 2.11 The result of the NDHM method.	19
Figure 2.12 Crack detection based on LBP features.....	20
Figure 2.13 Geometric crack as a gaussian function.	21
Figure 3.1 Different in size, location, and orientation, four beamlets	32
Figure 3.2 A weighted sum of pixel values along the lines' direction represents the beamlet transform.	33
Figure 3.3 Processing steps algorithm flowchart.....	34
Figure 4.1 Original of block crack image	35
Figure 4.2 Gray scale of block crack image.....	35
Figure 4.3 Enhancement of block crack image	36
Figure 4.4 Segmented of block crack image and threshold	36
Figure 4.5 Removed noise of block crack image	37
Figure 4.6 Crack length result for block crack.....	37
Figure 4.7 Residuals result for block crack.....	38
Figure 4.8 Original of longitudinal crack image	39
Figure 4.9 Gray scale of longitudinal crack image.....	40
Figure 4.10 Enhancement of longitudinal crack image	40
Figure 4.11 Segmented of longitudinal crack image and thresholding	41
Figure 4.12 Removed noise of longitudinal crack image	41
Figure 4.13 Crack length result for longitudinal crack	42
Figure 4.14 Residuals result for longitudinal crack.....	42

Figure 4.15 Original of transverse crack image	44
Figure 4.16 Gray scale of transverse crack image	45
Figure 4.17 Enhancement of transverse crack image	45
Figure 4.18 Segmented of transverse crack image and thresholding	46
Figure 4.19 Removed noise of transverse crack image	46
Figure 4.20 Crack length result for transverse crack	47
Figure 4.21 Residuals result for transverse crack	47
Figure 4.22 Original of alligator crack image	49
Figure 4.23 Gray scale of alligator crack image.....	50
Figure 4.24 Enhancement of alligator crack image	50
Figure 4.25 Segmented of alligator crack image and thresholding	51
Figure 4.26 Removed noise of alligator crack image	51
Figure 4.27 Crack length result for alligator crack.....	52
Figure 4.28 Residuals result for alligator crack.....	52

List of Tables

Table 3.1 The characteristics of different types of cracks	30
Table 3.2 Four main types of cracks used.....	30
Table 4.1 Block crack classification	38
Table 4.2 Longitudinal crack classification	43
Table 4.3 Transverse crack classification	48
Table 4.4 Alligator crack classification	53
Table 4.5 The Classification of success rate	54

List of Abbreviations

FCN:	Fully Convolutional Network
SVM:	Support Vector Machine
IoU:	Intersection over Union
ANN:	Artificial Neural Network
FC:	Fully Connected
ReLU:	Rectified Linear Unit
VOC:	Visual Object Classes
CNN:	Convolutional Neural Network
GPU:	Graphics Processing Unit
AASHTO:	American Association of State Highway and Transportation Officials
DIP:	Digital Image Processing
GIS:	Geographic Information System
NDHM:	Neighboring Difference Histogram Model
LBP:	Local Binary Patterns
ICIP:	International Conference on Image Processing
ROC:	Receiver operating characteristic
SVM:	Support Vector Machine
AUC:	Area Under characteristic
RCNN:	Region Convolutional Neural Network
MAP:	Mean Average Precision

CHAPTER I

Introduction

1.1 Background

Pavement cracks represent one of the most important issues in road maintenance, significantly affecting the structural integrity and service life of the road. These cracks, being the preliminary signs of various types of pavement diseases, are capable of inducing potential structural damages to the pavement, thus requiring early identification and timely repair (Ying & Salari, 2010). The current traditional methods of crack detection, while efficient to a certain extent, are marred by their inherent time-consuming nature, labor-intensive characteristics, and lack of accuracy, urging a necessity for more advanced methods for crack detection (Safaei et al., 2021).

In response to this need, recent years have seen a proliferation of scientific research aimed at leveraging modern technological advancements to achieve accurate and efficient extraction of crack information from images (Zhang et al., 2017). Numerous techniques for detecting pavement cracks have been published in the literature, including the valley bottom boundary extraction approach (Safaei et al., 2022) and the Prim minimal spanning tree-based crack connection algorithm (Localization & Techniques, 2022). However, in changing circumstances, these conventional procedures, which were created expressly for particular databases or scenarios, may not deliver satisfactory results.

Due to advancements in artificial intelligence, deep learning techniques are becoming increasingly frequently applied in the field of pavement crack detection (Hu et al., 2021). Although these techniques have significantly increased the effectiveness and accuracy of pavement crack detection (Zhang et al., 2017), a number of issues still exist, such as the dependence on complex feature extraction methods, the inability to adapt to different image sources or road sections, the impact of environmental factors on the stability and accuracy of algorithms, and the inability of current models to directly access road conditions (Alayat & Omar, 2023).

The current study proposes a novel strategy based on the combination of deep Beamlet transform Algorithm for pavement crack recognition in order to address these

drawbacks, with the aim of offering a general solution that can be applied in various crack detection circumstances. The simultaneous fracture detection and segmentation provided by this approach is a special benefit that boosts model (Zhao & Wang, 2010). The need of creating complex image processing algorithms to facilitate pavement crack inspection is underscored by the growing issues regarding pavement distresses. The use of moment invariant and neural networks (Zhao & Wang, 2010), the application of histogram projection (Ouyang et al., 2014), and the use of neural networks for crack detection and classification (Safaei et al., 2022) are just a few of the previous studies that have contributed to the field that are covered in-depth in this study.

1.2 Aim of the Study

The aim of this study is to developing an asphalt pavement crack detection and classification model by using beamlet transform algorithm. The objective is to improve crack detection's accuracy and effectiveness while also permitting classification of various pavement fracture kinds, facilitating prompt maintenance and repair activities.

1.3 Objectives of the Study

The study's particular goals are as follows:

- 1) Develop an image preprocessing technique to improve the visibility of pavement cracks.
- 2) Implement the Beamlet Transform Algorithm to effectively detect and segment pavement cracks in preprocessed images.
- 3) Extract pertinent features from detected cracks to enable classification into distinct types, including block cracks, alligator cracks, longitudinal cracks, and transverse cracks.

1.4 Problem Statement

Road maintenance is significantly hampered by pavement cracks, which also compromise the overall structural integrity of the infrastructure. Conventional crack detection techniques can take a long time, require a lot of labor, and are imprecise, which makes it difficult to plan effective maintenance. Furthermore, it is still difficult to classify various pavement crack kinds precisely. To enhance road maintenance and

increase the lifespan of asphalt pavements, it is urgently necessary to develop an advanced algorithm capable of accurately recognizing and classifying pavement fractures.

1.5 Research Question

How does the study use the Beamlet Transform Algorithm for accurate crack detection, feature extraction, model design, and evaluation on diverse asphalt pavement crack images?

1.6 Scope of the Study

The Beamlet Transform Algorithm is used in this study to construct a crack detection and classification model for asphalt pavement. The model's performance will be measured based on how well it can precisely identify and categorize various pavement fractures in the dataset used for the study.

1.7 Limitations

The accuracy and generalizability of the created model for detecting and classifying asphalt pavement cracks may be constrained by this study's limitations. The quality and diversity of the dataset used for training and evaluating the model may have an impact on how well it performs. The Beamlet Transform Algorithm may only be useful in detecting very narrow or minute cracks. Additionally, the effectiveness of the model may be impacted by outside variables like the illumination during image capture, and more investigation is required to determine whether it can be applied to other road and environmental changes.

CHAPTER II

Literature Review

2.1 Introduction

This chapter aims to review the previous studies and current practices in the domain of asphalt pavement crack detection and the classification model using the beamlet transform algorithm. The focus is on a broad range of methodologies, technologies, and systems that have been developed and used for applying the beamlet transform algorithm to classify asphalt pavement cracks. Additionally, the chapter will explore factors contributing to pavement cracks and potential strategies for prevention and maintenance.

2.1 Background in digital image processing

Digital image processing (DIP), which focuses on the manipulation, improvement, and interpretation of digital images to extract relevant information, has become a crucial area within computer vision and image analysis. DIP approaches have found use in a variety of fields, including medical imaging, remote sensing, surveillance, and infrastructure assessment, thanks to the growth of image capturing devices and the growing demand for automated analysis in numerous domains. The creation of reliable algorithms for crack identification and classification in various materials, particularly asphalt pavements, is one key difficulty that DIP addresses. (Ying and Salari 2010)

Digital image processing techniques have been intensively investigated by researchers in recent years as sophisticated tools to identify and categories cracks in asphalt pavements. The necessity of maintaining the integrity of the road infrastructure for reasons of economic and public safety is what motivates these efforts. There is a demand for automated ways because conventional manual inspection techniques take a long time and frequently lack precision. The use of DIP techniques, including as segmentation, texture analysis, and edge detection, has showed promise in more accurately and effectively locating and classifying fractures. (Ying and Salari 2010)

The Beamlet Transform (BT) is a novel method that has attracted interest in crack identification. Due to its capacity to record localized information in both the spatial and frequency domains, the Beamlet Transform, which was initially created for

seismic signal analysis, has been applied to a number of image processing tasks. This quality fits quite nicely with how uneven and varied pavement cracks are. By highlighting minute differences in texture, width, and direction, the BT method is intended to improve the accuracy of classification and better fracture detection (Ouyang et al., 2014).

The proposed model for asphalt pavement crack detection and classification using the Beamlet Transform algorithm addresses the limitations of conventional methods and offers the potential for more accurate, reliable, and automated assessment of pavement conditions. This research contributes to the broader field of digital image processing by showcasing the adaptability of sophisticated techniques like the Beamlet Transform in solving real-world infrastructure challenges. (Ouyang et al., 2014)

A 2D function with the notation $f(x, y)$ can be used to describe an image, where x and y stand for spatial coordinates. The coordinate pair (x, y) determines the location of a point or pixel within the image, while the value of f denotes the intensity (or colour) magnitude of the pixel (x, y) . The finite and discrete character of pixels and intensity levels establish the nature of images as digital data. (Gonzalez et al., 2002) describes the field of "Digital Image Processing" as including computer-based processing of digital images in the book "Digital Image Processing."

There is a divergence of opinions among scholars regarding the differentiation between image processing and allied fields such as image analysis and computer vision. the notion that images function as both input and output in image processing is a common one regarding these distinctions. However, Gonzalez et al. regarded this concept as "a limiting and somewhat artificial boundary" (Gonzalez et al., 2002). Building upon (Gonzalez et al., 2002), this dissertation explores these concepts.

It can be difficult to distinguish clearly between image processing and computer vision. Low-level, mid-level, and high-level processes are all types of computerized operations. At the lowest level, fundamental procedures that change images as inputs to produce equivalent outputs include contrast enhancement, noise reduction, and image sharpening. Mid-level procedures operate on image inputs to extract features like edges and contours. High-level processing, on the other hand, comprises complex

tasks like object recognition and detection that resemble the field of picture analysis (Zhao & Ning, 2017).

The three levels of computerized processes described previously are used in this dissertation to address various goals, including computer vision, complete image analysis, and image pre-processing. These endeavors encompass diverse undertakings such as object detection, segmentation, noise reduction, and the extraction of image features. The terminology "digital image processing" within this thesis pertains to procedures wherein images function as inputs and outputs, as well as procedures in which images serve as inputs, yielding outputs encompassing image features or feature recognition. The primary objective of these processes in this study is image analysis and recognition, utilizing state-of-the-art techniques such as machine learning (Eisenbach et al., 2017).

2.1 Cracking phenomenon understanding

The assessment of road conditions encompasses various metrics (Shahin & Kohn, 1979), with the cracking index serving as a vital instance that underscores the deterioration resulting from the emergence of fissures within the road surface.

According to a definition provided by the American Association of State Highway and Transportation Officials (AASHTO et al., 2018), a road crack is characterized as: "An interruption in the pavement surface with at least 1 mm width and 25 mm length." An alternate interpretation of crack, put forth by the PIARC Technical Committee Road/Vehicle Interaction, designates it as: "A disruption in the road surface marked by specified minimum measurements for length, width, and depth." Miller's technical report (Miller et al., 2014) comprehensively covers various crack types, encompassing facets like crack direction factor. These delineations collectively underscore that road surface cracks can be defined by four key attributes: length, width, depth, and orientation.

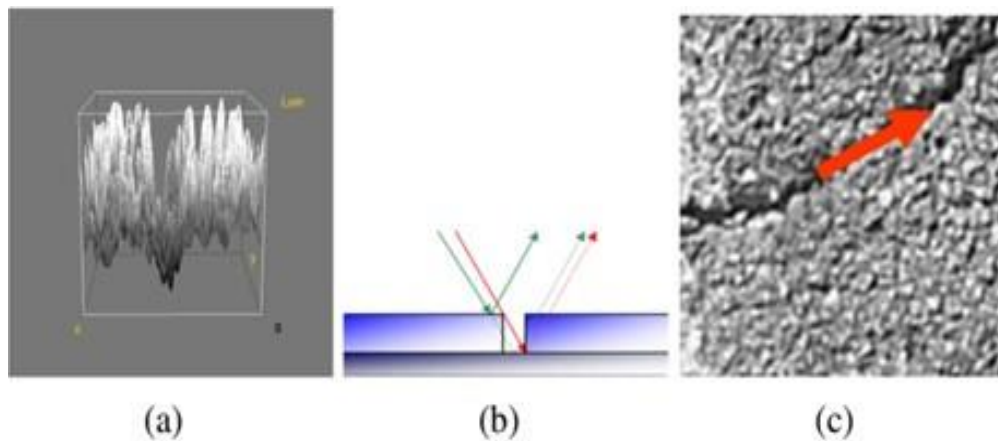
(Nguyen et al., 2009), in their exploration of crack identification and categorization, depicted road cracks in image representations based on the following attributes:

- Darker in comparison to the surrounding areas (attributed to the crack's form impeding the reflection of numerous light rays from the crack to the camera).

- Continuous in nature (with the crack potentially being lengthier or thinner than the particles around it).
- Predominant orientation (indicating a prevailing alignment that spans the entire crack or its individual segments).

Figure 2.1

Crack analysis on road images.



In subfigure (a), a graph illustrates the luminosity of an image featuring a crack within a three-dimensional coordinate system (x, y, intensity). Subsequently, subfigure (b) demonstrates two distinct lighting scenarios: one where light approaches the crack's edge and another where it emanates from the crack's bottom. Finally, subfigure (c) denotes the crack's orientation.

In his doctoral research, Oliveira defined various features of fractures in photographs based on crack direction, diameter, and length (Oliveira et al., 2013). Cracks should:

- Demonstrate linear progression in the specified direction.
- Display a specific width, such as equal to or greater than 2 mm.
- Have a significant length.

This article introduces a definition of cracks in pavement images, which applies to images with a spatial resolution of 1 pixel = 1 square millimeter or higher.

A crack can be defined by:

Length: Branch fractures or unconnected cracks have a minimum length of 25 pixels.

Intensity: For a 256-grey level - 8-bit image, a crack is darker than its surroundings by at least 5 grey levels.

Identifying whether a fracture is part of the interconnected network of road fractures or stands alone holds significant importance for maintenance endeavors. According to (Miller and Bellinger, 2014), an isolated crack with a length less than 300 mm (or 300 pixels in images) will not register as detectable.

Road maintenance methods, such as segmentation and fracture detection, are essential. To address this issue, a range of image processing techniques, both conventional and cutting-edge, are available. While conventional methods for fracture detection use edge detection or other low- or mid-level procedures, these techniques are susceptible to noise and undesirable artifacts in the road. Preprocessing image processes are necessary to improve accuracy before applying these procedures. Recently, systems utilizing machine learning approaches, such as deep learning, have been reported for identifying fractures in images. Some of these techniques demonstrate good performance, while others require preprocessing or involve non-standardized data collection approaches, and some are highly complex (Oliveira et al., 2013).

Even with substantial research efforts, the precision of existing methods for crack analysis, which aim to ascertain vital crack attributes like width, length, and orientation, frequently falls short. Moreover, these present techniques can inadvertently classify unrelated visual components as cracks, primarily due to the absence of a meticulous crack delineation. Addressing these constraints is complicated by the scarcity of reliable ground truth data of superior quality (Oliveira et al., 2013).

The subsequent portions will explore the current status of crack partitioning, categorization, and identification through the utilization of both two-dimensional (2D) and three-dimensional (3D) information, encompassing data formats like point clouds and visual representations. A range of techniques, spanning from conventional digital manipulation to advanced neural networks integrating machine learning methodologies, can be harnessed within crack analysis frameworks. The classification of road cracks can be conducted by considering their degree of seriousness or extent of deterioration (Oliveira et al., 2013).

2.3 Crack classification based on types of cracks

Crack occurrence represents a prevalent manifestation of degradation across road surfaces, encompassing both asphalt and concrete compositions, as expounded in the handbook for the long-term pavement performance program (Miller et al., 2014). Cracks can be systematically classified into six well-defined groupings (Miller et al., 2014).

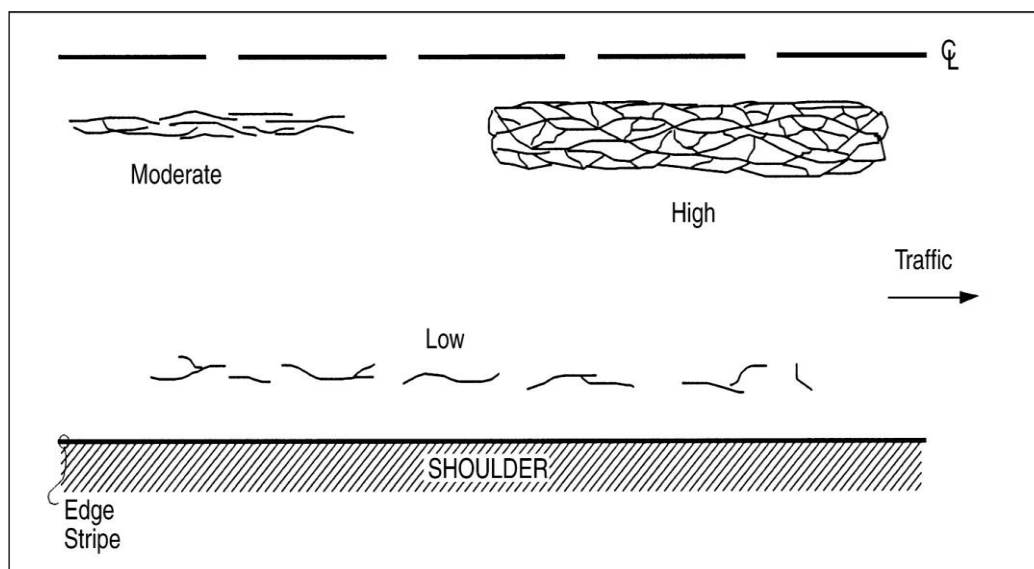
2.3.1 Fatigue cracks

Fatigue fractures, also known as alligator cracks due to their interconnected and alligator-skin-like appearance, are caused by traffic loading. These cracks often appear in areas where heavy trucks frequently traverse, leading to their development. The number of cracks per square meter can be used to calculate the density of these cracks.

Several instances of fatigue cracks are illustrated in Figure 2.2. It is evident from the examples that the severity of distress escalates with an increasing number of interconnections among the cracks.

Figure 2.2

Fatigue crack examples.

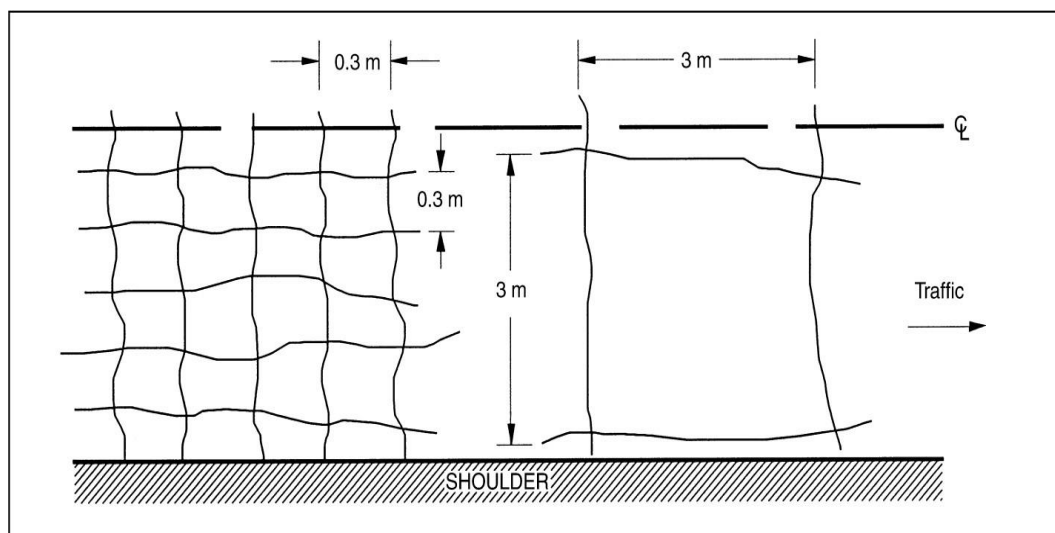


When cracks are closely related, it indicates a high level of severity. This specific type of crack lines up with the flow of traffic.

2.3.2 Block cracks

Figure 2.3

Block cracks.



Cracks that form longitudinally and transversely on the road surface tend to give rise to square-like segments. These segments, referred to as "block cracks," can vary in size, spanning from as compact as $0.3\text{m} \times 0.3\text{m}$ to as extensive as $3\text{m} \times 3\text{m}$.

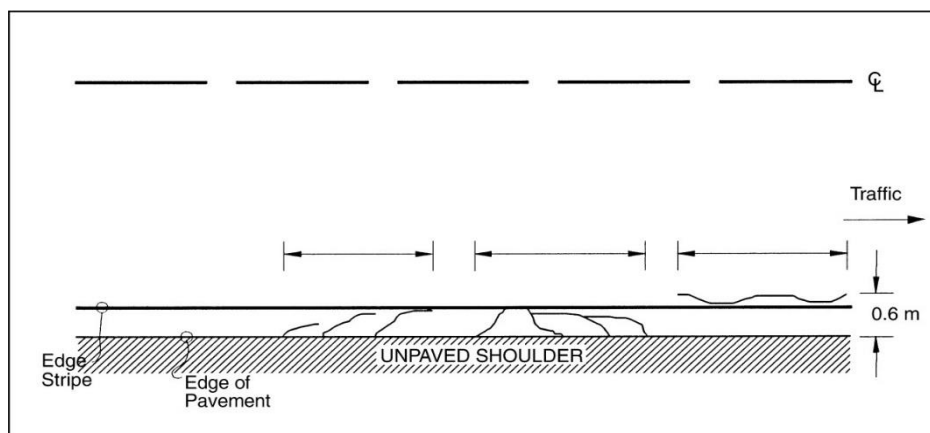
Block cracks result in the division of the road's surface into rectangular sections, where each rectangle covers an area spanning from 0.1 to 10 square meters. The emergence of block cracks is predominantly attributed to the "fatigue" phenomenon experienced by roads. Two instances of block cracks are depicted in Figure 2.3. On the left side, there are block cracks measuring $0.3\text{m} \times 0.3\text{m}$, while on the right side, there are block cracks measuring $3\text{m} \times 3\text{m}$. Smaller block crack sizes are indicative of more pronounced road distress.

2.3.3 Edge cracks

Edge cracks are characterized by their crescent-shaped pattern, originating from the road's edge and extending towards the shoulder. The extent of pavement edge influenced by these cracks can be quantified through length measurements. A representative instance of edge cracks is illustrated in Figure 2.10. It is plausible that the emergence of edge cracks is linked to the material fatigue experienced by the road surface.

Figure 2.4

Edge cracks



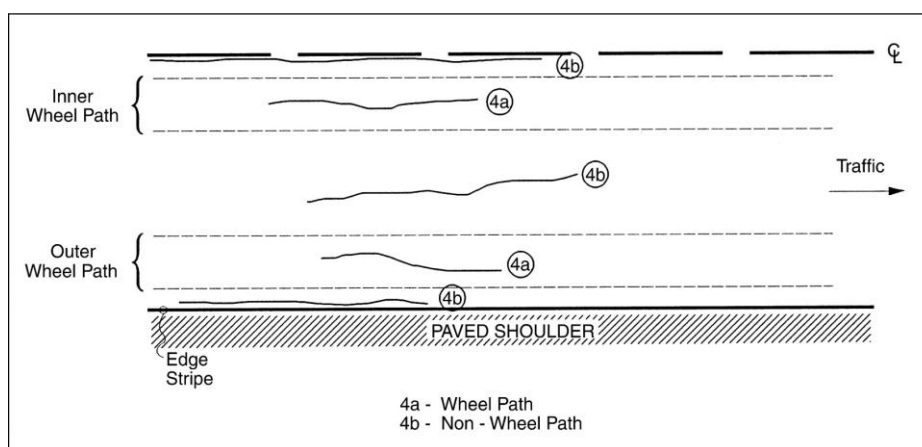
Edge cracks are indications of fissures near the unpaved road shoulder. The edge stripe and the outer edge of the pavement are connected by these fissures.

2.3.4 Longitudinal cracks

Longitudinal cracks are ones that follow the centerline of the road. These cracks must be positioned in the designated lane of the road since it is essential to distinguish longitudinal fractures from other kinds of cracks. Figure 2.5 shows two types of longitudinal cracks: those that are outside the wheel path and those that are found in the path of the wheels.

Figure 2.5

Longitudinal cracks.



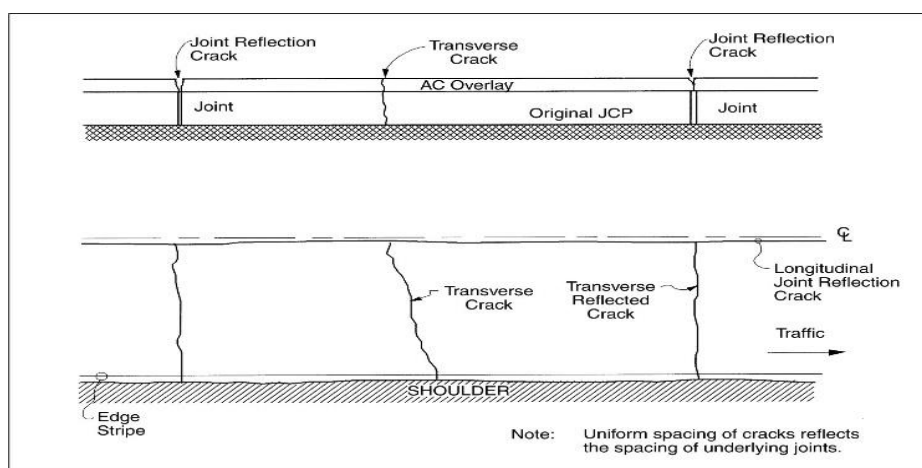
These go from the perimeter of the road towards its center and are positioned in accordance with the direction of traffic. The road surface is covered in fissures of this type.

2.3.5 Reflection cracks

Reflection fractures form on the concrete pavement's top layer, typically above joints. Figure 2.6 shows an instance of a reflection fracture. These cracks are the result of "reflection" damage stemming from the layer beneath the road surface. As such, they are associated with the joint of that underlying layer.

Figure 2.6

Reflection cracks.

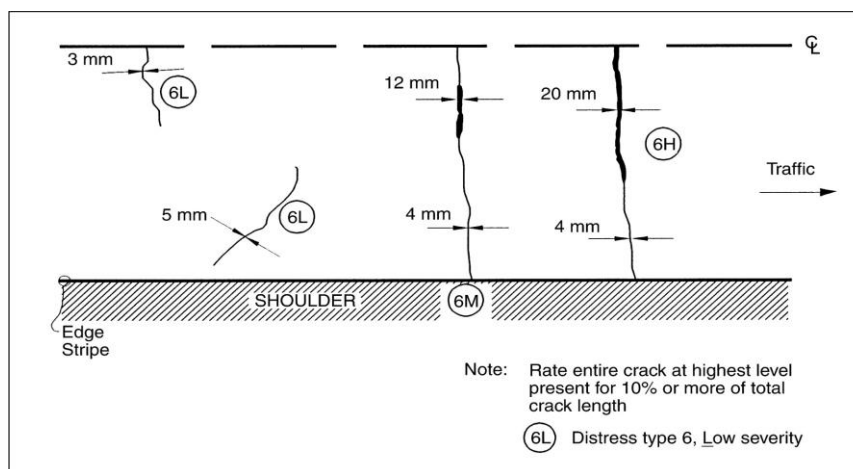


Reflection cracks arise when damage originates from a subsurface layer and is then mirrored by the uppermost layer of the road. These cracks share a visual similarity with transverse cracks in their outward appearance

2.3.6 Transverse cracks

The majority of transverse cracks are oriented perpendicular to the road's centerline. As illustrated in Figure 2.7, the width of transverse cracks can vary along their length. Thus, specifying the crack width should encompass the minimum, maximum, and average widths observed at different locations along the transverse cracks.

Engage in the practice of measuring road craters.

Figure 2.7*Transverse cracks.*

The width of cracks can be measured. Transverse cracks can vary in width, spanning from 3 millimeters to 20 millimeters.

2.4 Crack processing using traditional digital image processing

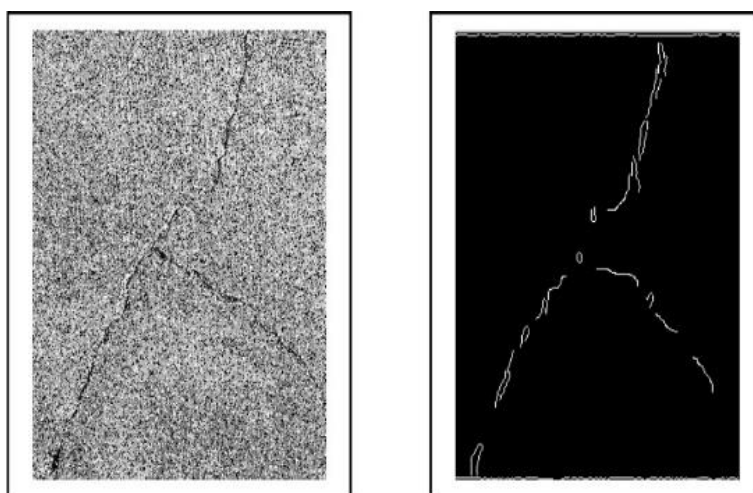
In conventional road maintenance practices, the identification and assessment of cracks have conventionally relied upon the expertise of road specialists or technicians operating under the guidance of experts. Nonetheless, this manual approach consumes a substantial amount of time and labor resources. Hence, the integration of automated or semi-automated approaches utilizing imagery has emerged as a prospective solution, aiming to streamline the evaluation of crack severity and overall road condition. A multitude of studies have been conducted, investigating the automated identification of cracks present on road surfaces (Li & Liu, 2008; Zakeri, Nejad, & Fahimifar, 2017). These research efforts underline the formidable challenge in crack detection, primarily attributed to the prevalent image noise and undesired artifacts, encompassing shadows, debris, and road markings. Moreover, in practical road assessment scenarios, images are captured by cameras affixed to swiftly moving vehicles, subjected to diverse environmental conditions (Zakeri, Nejad, & Fahimifar, 2017). Consequently, image quality fluctuates, posing a persistent challenge for reliable crack detection. It is important to note that a significant portion of advanced

methodologies addressing road crack concerns are confined to the realms of crack identification and categorization, often excluding the computation of crack indices.

There are two broad categories of crack detection, segmentation, and classification methodologies: those based on traditional Digital Image Processing (DIP) techniques, and those based on neural networks and machine learning paradigms. This section will provide a review of common techniques such as edge detection, Gabor filters, and picture feature extraction.

Figure 2.8

Improved canny method result.



The image on the left represents the original image, while the image on the right depicts the outcome generated by the Canny method. This approach effectively eliminates black-white dot noise present in the image; however, it falls short in maintaining the seamless continuity of cracks.

2.4.1 Edge detection

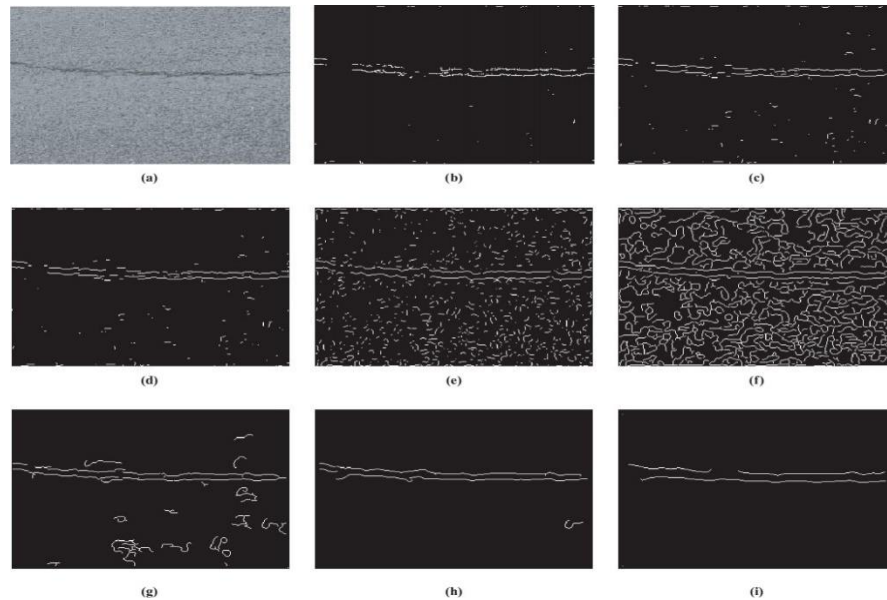
Traditional techniques in Digital Image Processing (DIP) commonly employ edge detection methods for identifying and categorizing cracks in asphalt pavements. Edge detection relies on the utilization of image gradients, specifically the first and second derivatives (Ziou & Tabbone, 1998). To enhance upon the Canny edge detection approach (Canny., 1987), various advancements have been proposed for detecting and characterizing cracks (Agaian et al., 2009; Zhao, Qin, & Wang, 2010). In the study by

(Huili Zhao and colleagues 2010), they enhanced road images by enhancing contrast before applying the Canny edge detection algorithm. This technique, suggested by Zhao, exhibits improved crack detection capabilities and is more effective in eliminating small noise artifacts compared to the conventional Canny method. Nevertheless, it struggles to eliminate other elements like zebra crossings or pavement signage. (Almuntashri and Papagiannakis, 2009) proposed an extension of the Canny method, known as AC test images, which fuses two edge detection outcomes. These images can be processed through a "Modified Canny kernel" or a combination of "Modified Canny kernel and Modified gradient Canny" to accentuate branch edges. However, the application of this technique to road images results in crack segments that are discontinuous, as illustrated in Figure 2.8.

Regarding conventional segmentation methods, a research paper examining crack segmentation (Tsai, Kaul, & Mersereau, 2010) For fracture identification, seven different edge detection algorithms were investigated. On 30 images, these techniques were evaluated, revealing that dynamic optimization yields the most promising outcomes. The experiments demonstrated that segmentation struggles to differentiate authentic cracks from similar features like paint. Wavelet transform is another foundation for edge detection, as exemplified in the works of (Aydin and Sankur, 1996) and (Porwik and Lisowska, 2004). Moreover, (Cuhadar and Tasdoken, 2019) harnessed wavelet transforms for assessing road conditions, building upon prior work in pavement condition evaluation using the same method (Cuhadar & Tasdoken, 2002). The International Roughness Index (IRI) and numerous other types of pavement condition data were used in this technique to show how adaptable the wavelet transform is as a segmentation tool.

Figure 2.9

Edge detection experimentation results for pavement image



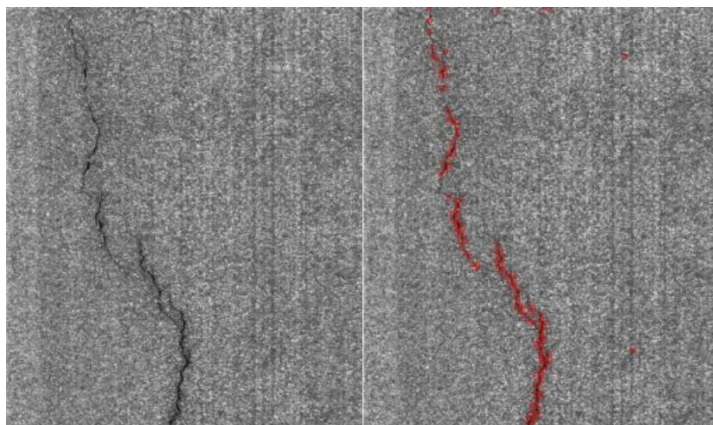
(a) Original image, (b) Robert edge detection, (c) Sobel edge detection, (d) Prewitt edge detection, (e) Laplacian of Gaussian (LOG) edge detection, (f) Canny edge detection, (g) Edges obtained using a trous algorithm with scaling 21, (h) Edges obtained using a trous algorithm with scaling 22, and (i) Edges obtained using a trous algorithm with scaling 23

However, this endeavor solely addresses data noise removal and necessitates reinforcement from the Geographic Information System (GIS). Wavelet-transform-based approaches were implemented as edge detection techniques for asphalt pavement images (Wang, Li, & Gong, 2007). (Wang and colleagues 2020) employed Mallat's algorithm (Mallat., 1989) as well as a trous algorithm to facilitate multi-resolution analysis, achieving commendable outcomes in the identification of longitudinal cracks and potholes. Nevertheless, their accomplishments were limited to specific road conditions and did not encompass a broader spectrum. A trous algorithm also requires an excessive amount of memory and processing resources. In conclusion, edge recognition is important, but it struggles with the large amount of noise in road photos that could mistakenly be identified as fractures. The performance of traditional edge detection filters and a trous method at various scales are compared in Figure 2.9.

Undoubtedly, a trous algorithm is excellent at reducing noise, but how effective it is depending much on the scaling parameter that is selected.

Figure 2.10

Gabor filter applied to a road image.



The image on the left represents the original image, while the image on the right illustrates the outcome obtained through the application of the Gabor filter technique (Salman et al., 2013). The identified cracks appear to be larger than their actual size.

2.4.2 Gabor filters

Gabor filters execute image filtering by relying on Gabor functions (Movellan et al., 2002). These filters are also employed for the extraction of image features (Ma, Wang, Tan, et al., 2002; Kong, Zhang, & Li, 2003). Gabor filters showcase effectiveness in the realm of texture segmentation (Salman et al., 2013), and considering road images' texture-rich nature, they prove valuable in the detection and segmentation of pavement cracks (Salman et al., 2013; Zalaama et al., 2014). In a crack detection proposal by (Bhoi and Solanki 2011), Salman introduced a set of Gabor filters with diverse orientations. The quantity of filters within a Gabor filter bank affects the output quality. While employing a greater number of orientations enhances accuracy, it concurrently leads to extended computational time and an increased false positive rate. This approach holds the advantage of capturing a majority of crack pixels, facilitating precise crack line segmentation. However, its susceptibility to noise is a limitation.

The outcomes of the Gabor method, illustrated in Figure 2.10, reveal that certain subtle cracks might not be detected (Bhoi & Solanki, 2011).

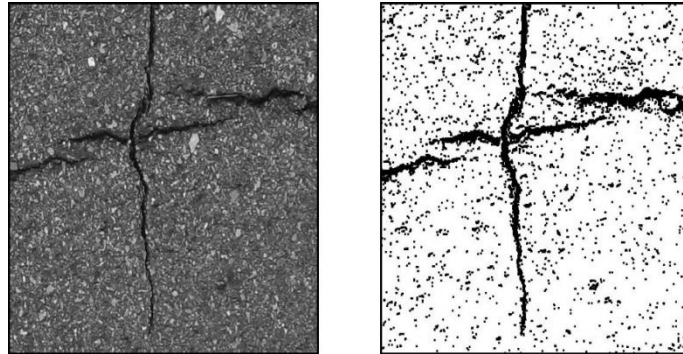
2.4.3 Adaptive thresholding

Adaptive thresholding is a method widely utilized in various applications within computer vision and graphics (Bradley & Roth, 2007). This method includes the comparison of each pixel with the average of its neighboring pixels while ignoring minor gradient fluctuations. In their proposal from 2007, Bradley and Roth introduced a technique known as the "integral image" with the intention of reducing the computational effort needed to compute the sum of pixels inside a rectangular area of an image. This approach is also used in a face identification proposal (Viola & Jones, 2004). A powerful image processing method that tackles fluctuations in lighting across space and removes noise is adaptive thresholding.

A variety of computer vision and graphic applications frequently employ the adaptive thresholding technique (Bradley & Roth, 2007). This approach ignores minute variations in gradients and evaluates each pixel in relation to the local average of its neighbours' pixels. The calculation of summed values within rectangular image regions was streamlined by (Bradley and Roth 2007) using an approach known as the "integral image," which is also used in face detection investigations (Viola & Jones, 2004). In image processing, adaptive thresholding shows to be a reliable approach for adjusting lighting fluctuations in space and reducing noise. In a separate study focused on crack detection (Fan et al., 2019), a deep Convolutional Neural Network (CNN) model was deployed by Fan and colleagues to identify regions containing cracks. Subsequently, an adaptive thresholding technique was implemented to segregate the detected cracks from the surrounding regions. This approach is notable for its simplicity and speed, boasting high accuracy particularly when handling images featuring prominent cracks. However, it remains limited in its inability to address dot-like noise, which is often prevalent in road image data.

Figure 2.11

The result of the NDHM method.



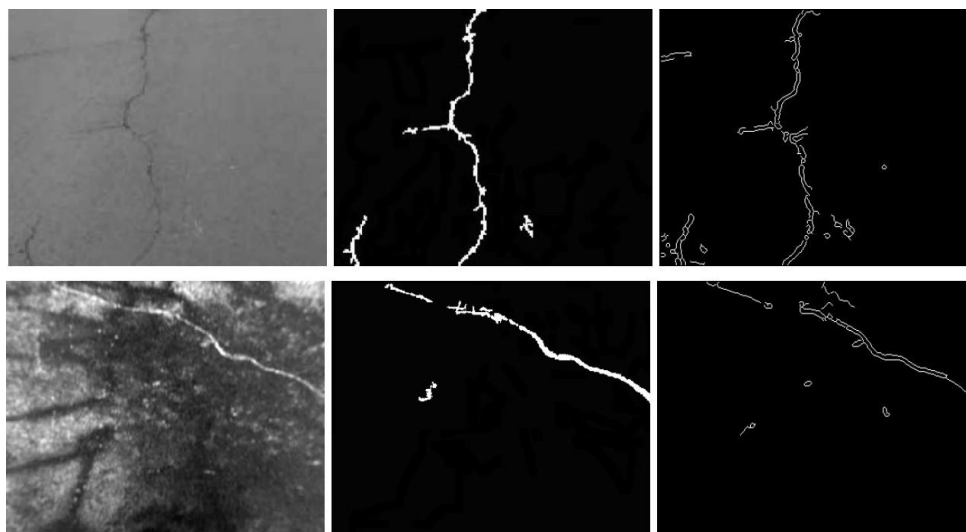
The original image is on the left, while the NDHM result is on the right. The presence of numerous black dots in the result illustrates the sensitivity of the NDHM approach to noise.

2.4.4 Crack detection based on image features

In the field of crack identification, attributes of images, such as the Neighboring Difference Histogram Model (NDHM) (Li & Liu, 2008), are helpful. The weighted contrast between the number of probable crack pixels and the number of nearby pixels is determined by the NDHM approach. The likelihood of designating a pixel as a crack pixel increases as the number of adjacent crack pixels grows. (Li and Liu, 2008) conducted a comparative analysis between their proposed method and classical thresholding techniques, including Otsu (Otsu et al., 1979) and Kapur (Kapur, Sahoo, & Wong, 1985), establishing the superior efficacy of the NDHM technique. Despite its adeptness at capturing almost all crack pixels, this method exhibits a tendency to detect noise, manifesting as dots and salt-and-pepper noise, as evidenced in Figure 2.11.

Figure 2.12

Crack detection based on LBP features.



The original images are displayed in the left column, the Hu result is displayed in the center column, and the Canny technique results are displayed in the right column. The Hu and Canny approaches classify the original image in the second row as a fracture even if it contains paint.

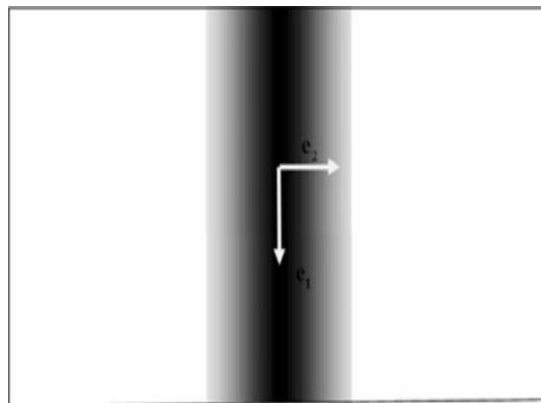
2.4.5 Geography features

Distinct geographic attributes have been harnessed for the purpose of detecting cracks in different materials (Nguyen, Kam, & Cheng, 2018). This approach has also been utilized in the context of road crack detection (Nguyen et al., 2014). In their work, (Nguyen and colleagues, 2014) conceptualized cracks as line-like structures exhibiting Gaussian cross-sectional intensity profiles, as depicted in Figure 2.13. Their methodology involves enhancing crack images using a Gaussian function-based filter and subsequently extracting the central crack line. Subsequent steps encompass the elimination of spurious cracks, including undesired edges. However, this technique necessitates preliminary and follow-up preprocessing stages to ensure accurate identification of authentic cracks.

In an effort to enhance crack detection, (Medina et al., 2014) proposed a technique that combines 2D images with 3D data processing methods. Their approach facilitates a detailed examination of cracks. The Median method employed by (Medina and colleagues 2014) involves extracting geometric information from road images. They achieved commendable balanced accuracies of 96% and 93% for transverse and longitudinal cracks, respectively. Prior approaches (Oliveira, 2013; Zou et al., 2012) have also employed crack attributes, such as width, curvature, and length, to distinguish crack pixels from non-crack pixels.

Figure 2.13

Geometric crack as a gaussian function.



A Gaussian function can be used to represent the intensity of a crack, with the center of the crack being the darkest value (lowest intensity).

In conclusion, these image characteristics are unsuccessful in fracture detection because road images are acquired under a variety of lighting and environmental situations. In essence, conventional image processing methods check differences in brightness between crack pixels and either the background or their nearby pixels. These techniques are frequently straightforward and demand little hardware. They are, nevertheless, sensitive to the noise and asymmetry found in images of roads. The methodologies that use neural networks in machine learning for object detection, road fracture detection, and segmentation are outlined in the next section. (Zou et al., 2012; Oliviera., 2013)

2.5 Background in machine learning

Machine learning involves the creation of computer programs capable of improving their performance through experience (Mitchell., 2006). When implementing a machine learning algorithm, an anticipated result can be represented as a function $y(x)$, where x represents the input data and y indicates the output vector, which is "encoded in the same way as the target vectors" (Svensén & Bishop, 2007). In the context of this thesis, specifically for detection and segmentation objectives, x takes the form of road crack data, including images or point clouds, while y assumes the shape of a $[1 \times 2]$ vector. The two values within the vector correspond to the two categories present in the input data, namely, crack and non-crack.

Machine learning algorithms can be broadly classified into three main types: supervised learning, unsupervised learning, and reinforcement learning. In supervised learning, human experts guide the algorithms by providing them with data along with corresponding labels. Conversely, unsupervised learning involves training without the use of labeled data. On the other hand, reinforcement learning (Sutton & Barto, 2018) observes the interaction between a given situation and the environment to make decisions that optimize rewards or minimize risks. In the context of this thesis, supervised learning is predominantly employed, where labels or ground truth data are provided by civil engineering experts.

Throughout this thesis, a wide range of machine learning algorithms are employed. However, the primary contributions arise from deep learning algorithms, specifically Convolutional Neural Networks (CNNs). The upcoming section provides a concise introduction to CNNs and their application in tackling object detection challenges.

2.5.1 Crack processing based on machine learning with convolutional neural networks

2.5.2 Crack detection

Deep learning constitutes a collection of machine learning methodologies that hinge on intricate layers of artificial neural networks. In the realm of crack identification and partitioning, neural networks assume a pivotal role. In this context, these models offer distinct benefits in comparison to conventional machine learning models (Zhang et al.,

2016; Fan et al., 2018; Nguyen et al., 2018). Deep learning models possess the inherent capability to autonomously grasp features embedded within images, a task that traditional machine learning methods necessitate users to manually engineer image features for. Moreover, deep learning excels in capturing subtle defects that prove arduous to train, such as minor aberrations in product labeling. Recently, the field of deep learning has emerged as a formidable approach employed to tackle the challenges of detection and segmentation. A comprehensive analysis of twelve techniques for crack detection unveiled that half of them are rooted in neural networks, encompassing both unsupervised and supervised methodologies (Oliveira et al., 2013).

In the field of asphalt pavement crack detection and classification, two main methodologies are identified: pixel-based crack detection and block-based crack detection. Although the block-based approach achieves an approximate accuracy of 90%, its efficacy is contingent on complex data preprocessing prior to training and testing (Zhang et al., 2016; Fan et al., 2018; Medina et al., 2014; Maeda et al., 2018).

In a study presented at the International Conference on Image Processing (ICIP), (Zhang et al., 2016) employed a Convolutional Neural Network (CNN) to detect cracks in images. Notably, the images in this study were captured using smartphones, differing from data sourced from practical systems, which typically involve monochromatic images obtained using specialized high-speed cameras. According to Zhang's methodology, a positive sample is defined as a patch that is centered within a 5-pixel radius of the crack centroid and a negative sample is a patch that is completely clear of cracks.

To evaluate the performance of their proposed model, the authors conducted a comparative analysis of the Receiver Operating Characteristic (ROC) curve using a Support Vector Machine (SVM) (Chang & Lin, 2011), a Boosting algorithm (Freund, Schapire, & Abe, 1999), and their own model. The findings highlight their model's highest Area Under the ROC Curve (AUC) of 0.845. Nevertheless, the final F1 score of 89% achieved by the proposed model is relatively moderate for crack detection issues, with detected cracks often larger than actual cracks. It's noteworthy that Zhang's model employs a substantial number of kernels (48 kernels per CNN layer), potentially leading to prolonged CNN training times.

(Maeda et al., 2018) conducted a comprehensive study on various deep learning and convolutional network approaches for detecting road damage and cracks in images. They curated a novel dataset using a smartphone mounted on a moving vehicle, spanning eight categories of road damage, including five types of cracks.

Regarding another study by (Fan et al., 2018), a CNN model was employed to analyze two publicly available road crack datasets, CFD and AigleRN. The datasets were used without preprocessing to address the challenge posed by imbalanced data. Fan's architectural design consisted of nine layers, including two CNN layers with 16 kernels each, max-pooling, two CNN layers with 32 kernels each, and three fully-connected layers. The model achieved a commendable final score exceeding 90%. However, it relied on a multi-label classification model, requiring post-processing for crack differentiation, and its limited training images carried the risk of model instability.

(Zhang et al., 2017) introduced a CNN model for 3D pavement crack data, displaying impressive accuracy on sound data but struggling with faint cracks and input disturbances. On a similar note, the model presented by (Fan et al., 2018) might not adapt well to noisy and artifact-ridden low spatial resolution images.

In the realm of automated crack detection and classification, YOLO v2 (Mandal et al., 2018) was employed, achieving an F1 score of 0.87 but lacking pixel-level segmentation. RetinaNet (Ale et al., 2018), another deep learning-based model, also tackled road damage detection, albeit with limitations in recognizing certain artifacts as cracks.

In a bid to rapidly identify cracks, (Park et al., 2019) proposed a two-module model that demonstrated impressive precision and recall. However, challenges arose when processing images containing both cracks and road markings or border-placed cracks.

In conclusion, CNN designs for fracture detection share the following common characteristics:

- Input data comprises both affirmative and negative instances. Positive instances encompass crack pixels positioned at the center, while negative instances lack any crack characteristics.

- Architectures for Convolutional Neural Networks (CNNs) with three to five convolutional layers are frequently used for crack detection. Each convolutional layer's kernel count can either stay constant over time or gradually rise from the first to the last.
- Incorporating max-pooling layers aids in reducing the number of parameters within the network.
- The ultimate layer utilizes a SoftMax activation function. This fully connected layer consists of two neurons, tasked with classifying the input image into either the crack (positive) or non-crack (negative) category.

Prior studies can be regarded as sample-level crack detection, where evaluations are conducted at the visual region level rather than assessing pixel-level categorization accuracy. To pinpoint fractures at the pixel level, specific segmentation techniques at the image's smallest unit are recommended. The subsequent section will cover the methodologies employed for pixel-level crack detection and crack segmentation.

2.5.3 Crack segmentation

This section provides an overview of certain studies that initially employed CNNs for general object segmentation, followed by an exploration of research focused on crack segmentation.

An initial investigation delves into CNN utilization for comprehensive object segmentation. Subsequently, the inquiry shifts to studies specifically addressing crack segmentation.

A study by (Girshick et al., 2014) introduced the Region-Based Semantic Segmentation (R-CNN) technique. This innovative approach employs CNN features to detect and segment images based on distinctive regions. R-CNN is made up of three main parts: the first stage produces about 2000 category-neutral region proposals; the second stage uses a large CNN to extract feature vectors from each region; and the third and final stage uses a linear algorithm, like a Support Vector Machine (SVM), to classify regions. On the VOC2012 dataset, Girshick's model achieves a mean Average Precision (mAP) of 53.3%. Nevertheless, Girshick's proposal highlights certain drawbacks, including substantial memory requirements and sluggishness during training and testing phases (Girshick et al., 2014).

Fast R-CNN, an advancement over R-CNN by (Girshick et al., 2015), streamlines computation by sharing resources during object proposal convolutional network forward passes. Fast R-CNN introduces two notable improvements. In order to extract feature vectors from the feature map, it first incorporates regions of interest (RoI) into the pooling layer. Two sibling layers are included in the output, one for predicting object classes and the other for fine-tuning object bounding box placements. In contrast to R-CNN and SPPNet, the training and testing phases are noticeably shortened (He & Sun, 2015). However, the use of selective search computing remains essential for enhancing training speed (Girshick et al., 2015).

Mask R-CNN, an extension of Faster R-CNN, was introduced by (He et al., 2017) to facilitate pixel-level segmentation. A distinctive feature of Mask R-CNN is the simultaneous integration of a mask component alongside the existing branch for bounding box recognition. He et al. also introduces RoIAlign, a pixel-to-pixel alignment method that mitigates the issues associated with RoI pooling layer quantization and aligns extracted features with input data. While Mask R-CNN achieves precise pixel localization for objects, it remains less effective in segmenting small objects (He et al., 2017).

Building on the information from VGG16 (Simonyan & Zisserman, 2014), (Long et al., 2015) presented Fully Convolutional Networks (FCN) for semantic segmentation. VGG16's fully connected layers are converted into convolutional layers by FCN using a 1x1 convolutional layer, allowing the classification network to produce low-resolution heatmaps. These semantic feature maps serve as input for up-sampling via transposed convolutions. This up-sampling process is progressively refined across stages. FCN accommodates inputs of varying sizes and yields corresponding-sized outputs. Although FCN excels in spatial information extraction and attains a higher mean Intersection over Union (IoU) compared to other segmentation nets like R-CNN, its complexity and time-consuming training due to the numerous convolutional layer kernels are noteworthy (Long et al., 2015).

In the beginning, U-Net was developed to segment biological images (Ronneberger et al., 2015). Its use has been expanded to include numerous additional image segmentation tasks. A contracting segment for feature computation and an expanding segment for localizing patterns in the image make up the two main components of the

U-Net architecture. The contracting section employs max-pooling layers to decrease parameters and picture dimensions while the expanding section uses up-pooling layers to increase image size, producing an output image that is the same size as the original image. Concat layers integrate feature maps at the same level in both components of the U-Net design, improving object localization precision. There are a total of 23 convolutional layers in the network. The cornerstones of Ronneberger's methodology are the overlap title and separation of touching items procedures. While the remaining technique trains the network to recognize minute borders separating adjacent cells, the Overlap Title strategy uses the U-Net model to anticipate various portions of the entire image. On the ISBI cell tracking task, Ronneberger's U-Net earns a remarkable Intersection over Union (IoU) score of 0.9203 (Ronneberger et al., 2015).

SegNet is a deep convolutional encoder-decoder architecture developed for image segmentation, according to (Badrinarayanan et al., 2017). Both indoor and outdoor scene prediction have been done using it. The first 13 levels of the VGG16 network are replicated in the encoder network's 13 convolutional layers (Simonyan & Zisserman, 2014). This produces a collection of feature maps, which the relevant decoders then up-sample. Notably, SegNet uses a method that reduces the number of parameters by just storing max-pooling indices. SegNet performs equally well as FCN while consuming less RAM. For the majority of objects, it outperforms other techniques in border delineation.

Another convolutional neural network (CNN) that is used for the segmentation of medical X-ray images is XNet (Bullock et al., 2019). The encoder-decoder architecture used by XNet is typical for applications involving picture segmentation. XNet manages to achieve a remarkable overall accuracy of 92% and an AUC of 0.98 despite training on a relatively small dataset of 108 photos encompassing 10 body parts. The serial down-sampling component of the X-Net encoder is smaller than that of other segmentation networks, which makes it unique. Two encoder-decoder modules are also used by the authors to improve feature extraction without significantly lowering image resolution. Over three categories of X-ray images, XNet routinely achieves F1-Score and AUC scores above 90%. XNet has a higher F1 score overall than SegNet, although using fewer parameters, according to a comparison study comparing the two networks (Bullock et al., 2019).

As per (Liu et al., 2019), Deep Crack represents a distinct model employing a deep hierarchical neural network for fracture segmentation. The researchers propose the utilization of a deep hierarchical CNN for the segmentation of fractures at the pixel level. To generate substantial side-outputs across different scales, Deep Crack employs the initial 13 layers, akin to VGG-16, while omitting fully connected layers and the fifth pooling layer, thus leading to reduced memory usage and computational time. This is achieved through the incorporation of a guide filter inspired by guided feathering, enhancing final predictions and diminishing noise in low-level predictions (He et al., 2012). The dataset comprises over 500 images sourced from the internet and the authors' personal collection, introducing real-world challenges owing to variations in spatial resolutions and features among these images. The effectiveness of the Deep Crack model in fracture segmentation is evident from its mean Intersection over Union (IoU) of 85.9 and an F1 score of 86.5% (He et al., 2012).

In conclusion, the image segmentation architectures mentioned above frequently exhibit the following characteristics:

- The methods incorporate the network architecture's backbone. The two symmetrical components of this backbone often involve encoding and decoding or contracting and expanding.
- Some approaches introduce a novel design for the decoding portion while utilizing existing networks for the encoding portion, such as VGG16 (Simonyan & Zisserman, 2014).
- These methods utilize concatenation layers.
- The techniques employ the projection layer or feature map pooling, also known as the convolutional 1x1 layer, for channel-wise pooling.

While a limitation of crack detection techniques is their tendency to identify only portions or limited regions containing cracks, resulting in the detection of cracks larger than their actual size (Nguyen et al., 2018; Zhang et al., 2016), crack segmentation methods face challenges due to the varying resolutions of road images and the presence of numerous artifacts, notably challenging-to-remove noise. As a solution, recent advancements have adopted a two-stage framework, combining both crack detection and segmentation within a single architecture. The following section will delve into an exploration of these novel approaches that leverage a two-stage design.

CHAPTER III

Methodology

3.1 Overview

This chapter discusses the method used in the asphalt pavement crack detection using beamlet transform algorithm method. The methodology specifies a step-by-step process for precisely recognizing and classifying pavement cracks. It encompasses image preprocessing, crack detection, and crack classification.

3.2 Crack classification standard

This thesis utilizes images procured from cement and asphalt roads, which are accessible at <https://github.com/cuilimeng/CrackForest-dataset>. A quantitative analysis of 1000 images' worth of data was conducted. Generally, images of asphalt pavement crack detection display linear attributes and are often discontinuous due to considerable environmental interference. This aspect makes it challenging for traditional pixel-based methods to effectively detect and categorize these cracks. However, the Beamlet algorithm proves robust in its line detection capabilities, making it suitable for crack detection and classification tasks (Ouyang et al., 2014).

When acquiring images for the purpose of detecting cracks in asphalt pavement, the cracks are projected onto both horizontal and vertical planes, thereby facilitating measurements. By assessing the count of branches and their orientation in the horizontal dimension, it becomes feasible to classify a given crack. As indicated in Table 3.1, the cracks fall into four primary categories: block cracks, alligator cracks, longitudinal cracks, and transverse cracks. The angle of each crack is calculated from its initiation point to its termination point. Irrespective of its angle, the presence of a branch identifies a block crack. The summation of the lengths of individual blocks along a crack corresponds to the overall crack length, with the length of a block crack being defined as the highest value of the Beamlet transform within each cell block of a crack image (Ouyang et al., 2014).

Table 3.1*The characteristics of different types of cracks*

Types of cracks	Crack angle Ω	Branches
Block	$\Omega \geq 60^\circ$	NO
Longitudinal	$\Omega \leq 30^\circ$	NO
Transverse	$60^\circ > \Omega > 30^\circ$	NO
Alligator	-	YES

3.3 Method

The Beamlet Transform Algorithm is used to analyze images of pavement cracks in the recommended method. The images are preprocessed to enhance crack visibility and then subjected to the Beamlet Transform for detection and segmentation of cracks. Relevant features are extracted from the detected cracks, and a classification model is trained to classify the cracks into four main types.

Table 3.2*Four main types of cracks used*

Crack Types	Images
Block	250
Longitudinal	250
Transverse	250
Alligator	250

3.3.1 Beamlet transform algorithm image processing

Image preprocessing is a critical preliminary step in the process of detecting and characterizing cracks in asphalt pavement images. The journey begins with the original image, capturing the real-world pavement conditions. To facilitate focused analysis, the next step involves converting the image into grayscale. The method then simplifies processing by isolating the intensity variations that include crucial information about characteristics like cracks. (Safaei et al., 2021)

Image enhancement techniques are used to further improve the image's quality. These methods alter brightness and contrast to make sure that minute details, like cracks, stand out against the background. This phase is essential to enhancing the algorithm's capacity to recognize elements precisely even in poor lighting situations. (Safaei et al., 2021)

The programme then continues by applying thresholding techniques to segment the image. By dividing the image into multiple zones, this makes it easier to separate interesting areas possibly cracks from the background. The algorithm can concentrate its efforts on the important areas of the image thanks to this segmentation, which provides a framework for further research. (Ying & Salari, 2010)

Real-world photographs invariably contain noise, which can make accurate analysis difficult. The program me uses noise reduction techniques to lessen its effects. These methods purge the image of undesired artefacts and disruptions, enhancing the signal-to-noise ratio. The program me improves its capacity to precisely identify and characterize cracks by reducing noise. (Duc et al., 2018)

As a crucial result, the program me measures crack lengths. The findings help with assessment and management of the pavement by offering useful information about its state. The technique sets the foundation for accurate and reliable crack identification and characterization through meticulous preprocessing procedures, enabling more informed decisions about pavement management and maintenance. (Duc et al., 2018)

3.4 Beamlet algorithm

3.4.1 Beamlet dictionary

The implementation of the beamlet transform occurs within image sections that are dynamically divided into squares. Visual representations of images occur within the continuous square $[0, 1]^2$, in this scenario, pixels are arranged in a grid of $1/n$ by $1/n$ squares throughout the $[0, 1]^2$ area. The compilation of beamlets constitutes a diverse range of line segments, encompassing a broad spectrum of orientations, positions, and scales. This variation is visually portrayed in Figure 3.1

3.4.2 Beamlet transform

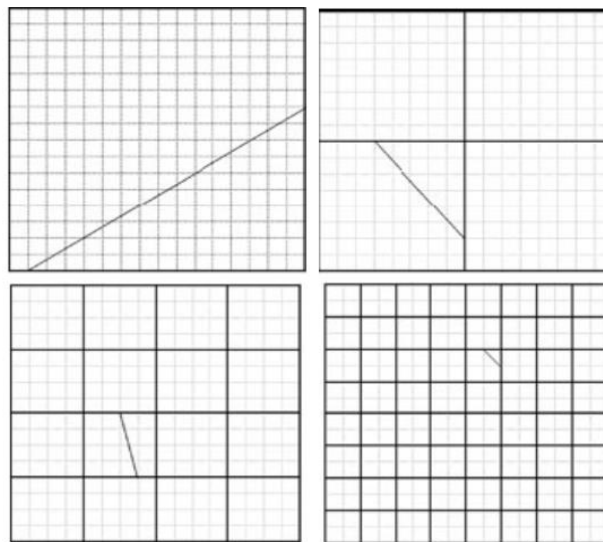
The beamlet transform is characterized as the summation of line integrals calculated across the entirety of the beamlet set. Consider $f(x_1, x_2)$ to be perceived as a continuous function within a two-dimensional space, where x_1 and x_2 denote coordinates (Ouyang et al., 2014). The beamlet transform T_f of the function f is outlined as follows:

$$T_f(b) = \int_b f(x(l)) dl, b \in B_E$$

Here, B_E represents the total collection of beamlets.

Figure 3.1

Different in size, location, and orientation, four beamlets

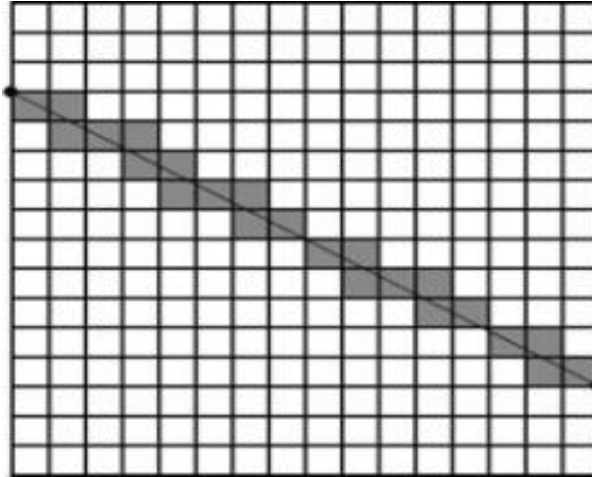


In the context of digital images, the beamlet transform evaluates the line integral within the discrete domain. As depicted in Figure 3.2, the depiction of the beamlet transform for all points along beamlet b is articulated in the following manner:

$$f(x_1, x_2) = \sum_{i_1, i_2} f_{i_1, i_2} \Phi_{i_1, i_2}(x_1, x_2)$$

Figure 3.2

A weighted sum of pixel values along the lines' direction represents the beamlet transform.



Where f_{i_1, i_2} refers to the gray level value of the pixel located at (i_1, i_2) and $\Phi_{i_1, i_2}(x_1, x_2)$ stands for the pixel's related weight function. Multiple options are available for the selection of $\Phi_{i_1, i_2}(x_1, x_2)$, and In this study, the average interpolation function is the one we choose. (Ouyang et al., 2014).

If $p(x_1, x_2)$ represent $[i_1/n, (i_1 + 1)/n] \times [i_2/n, (i_2 + 1)/n]$, choose function Φ_{i_1, i_2} fulfill the equation:

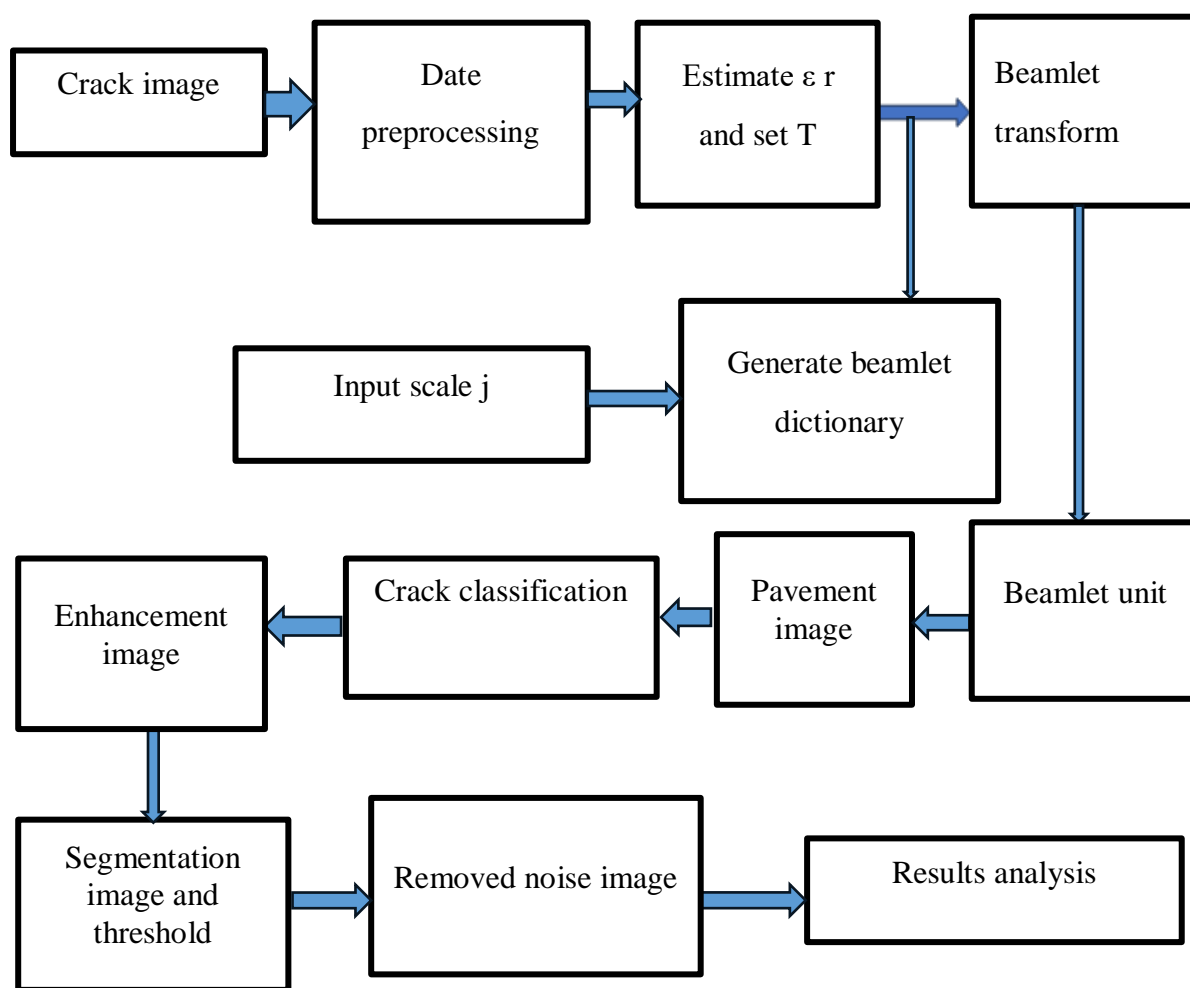
$$n^2 \int_{P(x_1, x_2)} \Phi_{i_1, i_2}(x_1, x_2) dx_1 dx_2 = \delta_{i_1, i_2}$$

3.4.3 Algorithm flow

Beamlet transform can be used to identify images based on pavement crack features; Figure 3.3 shows the fundamental method.

Figure 3.3

Processing steps algorithm flowchart



CHAPTER IV

Result and Discussion

Asphalt pavement crack detection image was treated using the steps of image enhancement, segmented image, thresholding, eliminated denoising processing, and image improvement according to the algorithm flow (figure. 3.4). The results are displayed below. The following images display the outcomes of applying the Beamlet algorithm to the various types of pavement crack images.

Figure 4.1

Original of block crack image



Figure 4.2

Gray scale of block crack image

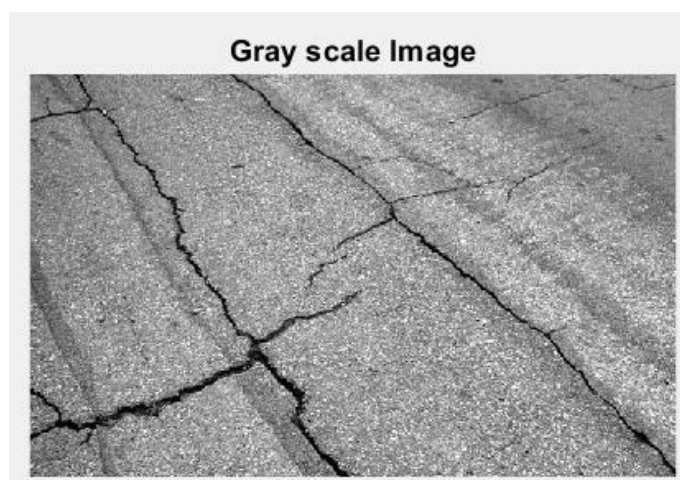
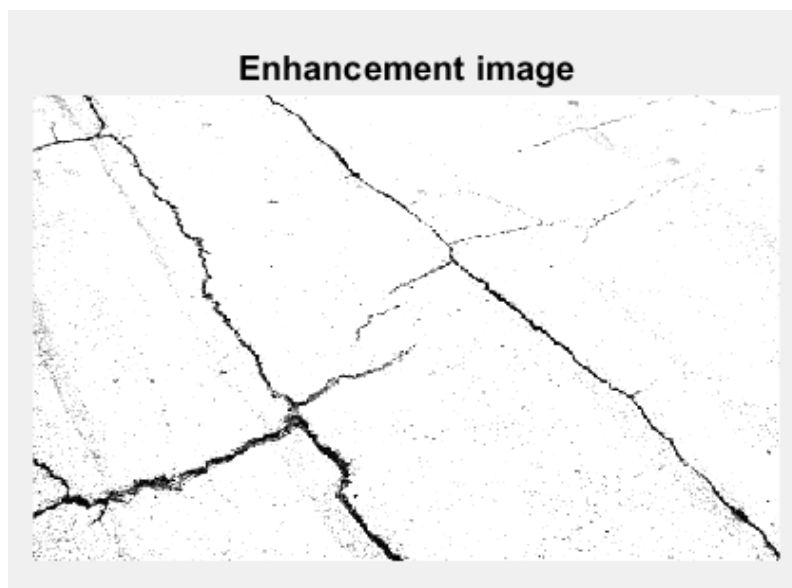


Figure 4.3

Enhancement of block crack image

**Figure 4.4**

Segmented of block crack image and threshold

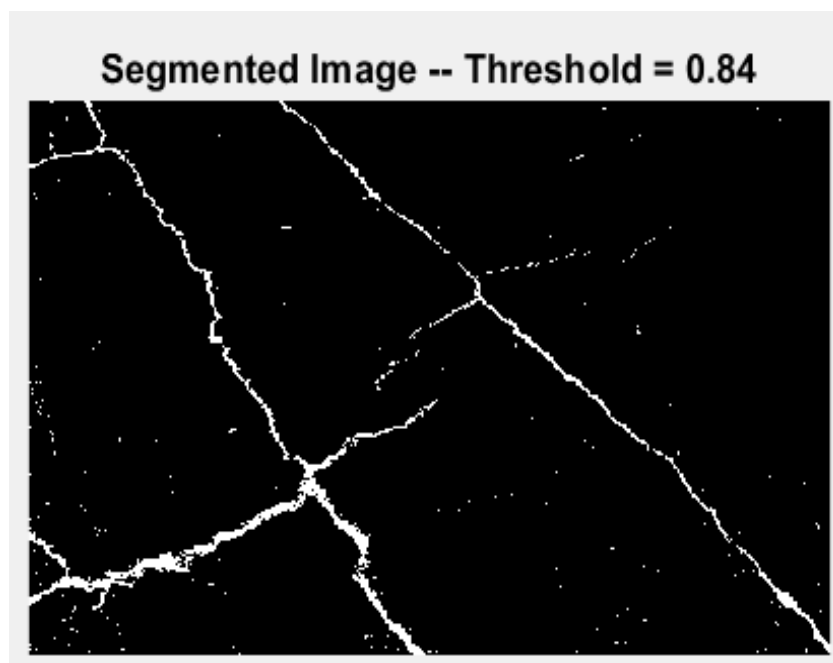
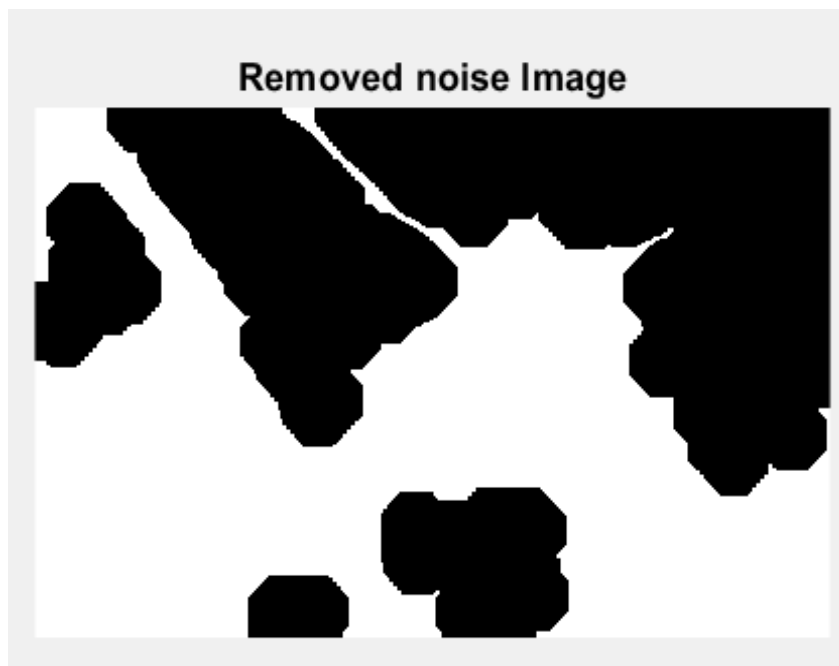


Figure 4.5

Removed noise of block crack image

**Figure 4.6**

Crack Area result for block crack

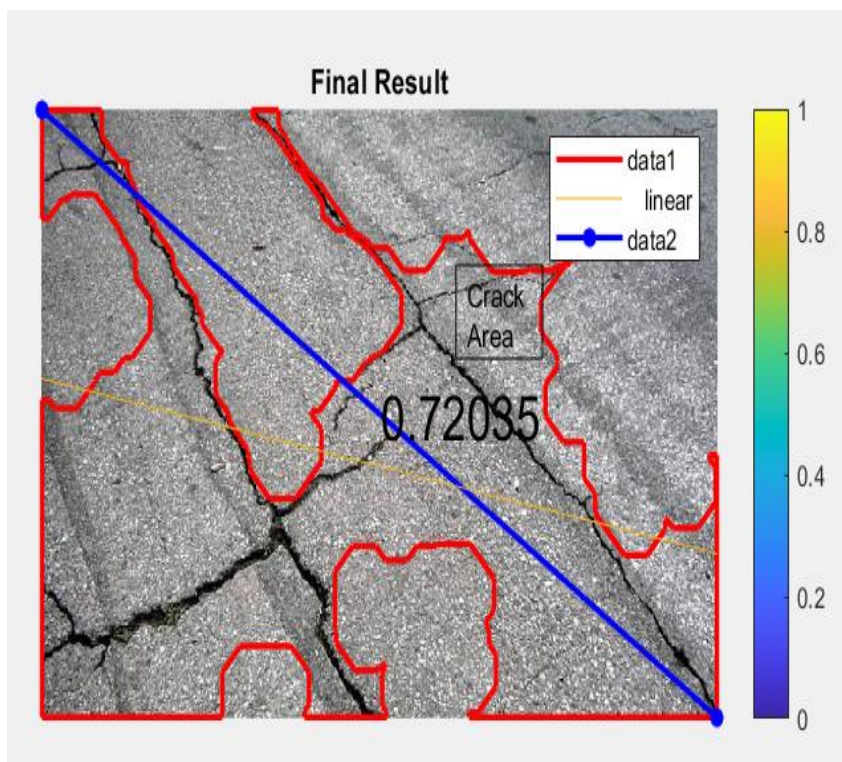
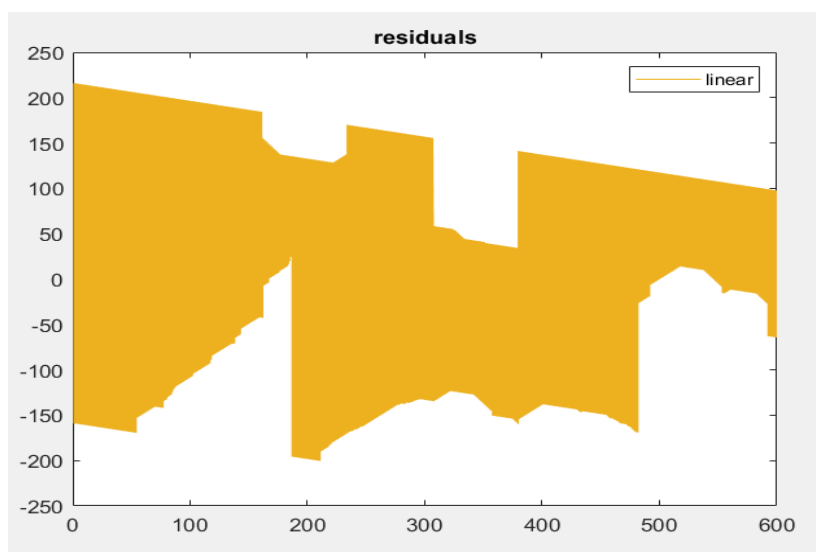


Figure 4.7*Residuals result for block crack***Table 4.1***Block crack classification*

Number	Crack angle Ω	Crack Area	Threshold	Branches	Crack types
1	-	0.72035 m ²	0.84	Yes	Block

The original image was changed into a single-channel image to create the grayscale image in Figure 4.2. This conversion facilitates better feature extraction and streamlines the future stages of image processing.

An image enhancement technique was used, as illustrated in Figure, to improve the fracture details. The fractures became more visible and distinct from the background thanks to this technique, which also increased their visibility and clarity.

The fractures were then represented as a binary image by segmenting the image using a thresholding technique with a threshold value of 0.84 in Figure 4.4. By segmenting the pavement, the fracture sections were separated from the remainder of the pavement surface.

A denoising technique was used to eliminate noise and artifacts from the segmented image, creating the denoised image depicted in Figure 4.5. The accuracy of the succeeding fracture detection and classification phases was enhanced by the elimination of noise.

The block crack under study has a final crack Area measurement of 0.72035 m^2 as a consequence of the fracture detection and classification process. It was discovered that the crack. These measurements were made by looking at the denoised image and using the right crack feature extraction tools.

An overview of the block crack classification findings is shown in Table 4.1. For each crack, the analysis's threshold values, crack length, and crack angle are provided. Based on the acquired measurements and threshold criteria, the fracture in this instance was identified as a block crack.

The beamlet transform algorithm was used to construct an algorithm for the detection and classification of block cracks in asphalt pavement, and the results showed great promise. During the image processing processes, the model successfully preserved the fracture information and correctly separated the cracks from the background. In order to determine the model's generalizability and dependability in practical circumstances, additional testing and validation of its performance on a bigger dataset would be beneficial.

Figure 4.8

Original of longitudinal crack image

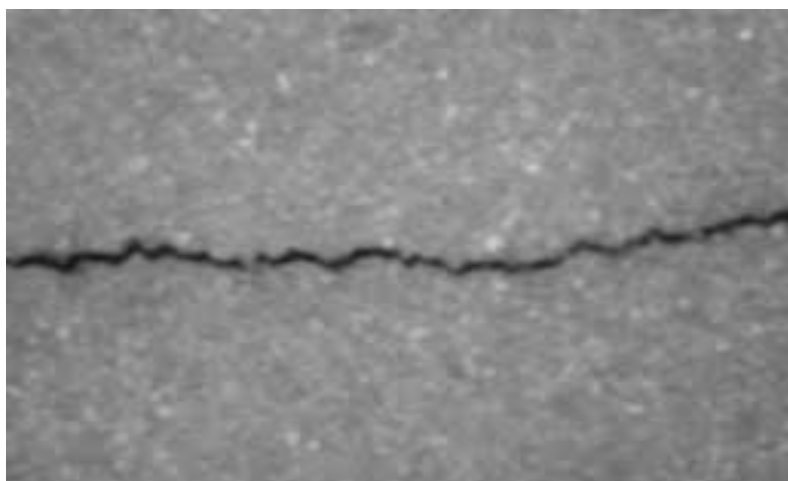
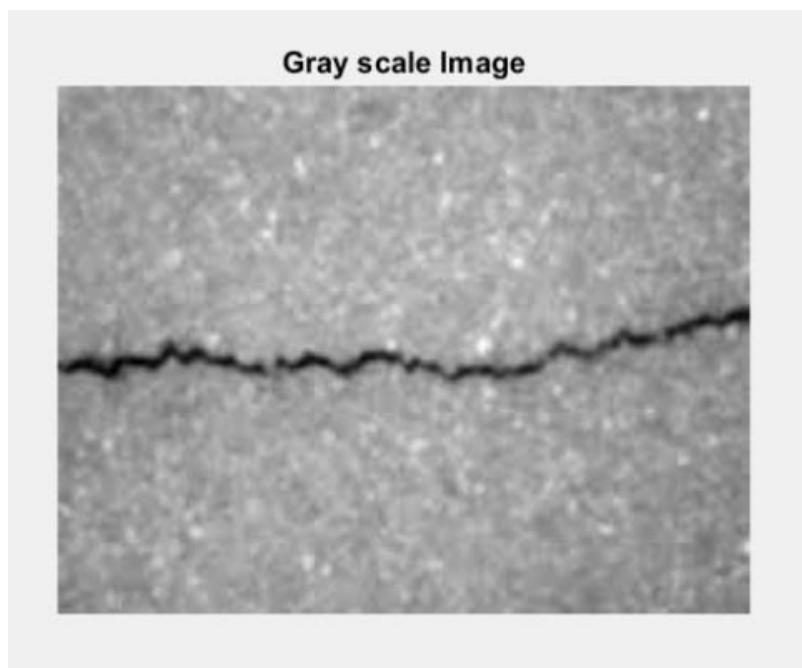


Figure 4.9

Gray scale of longitudinal crack image

**Figure 4.10**

Enhancement of longitudinal crack image

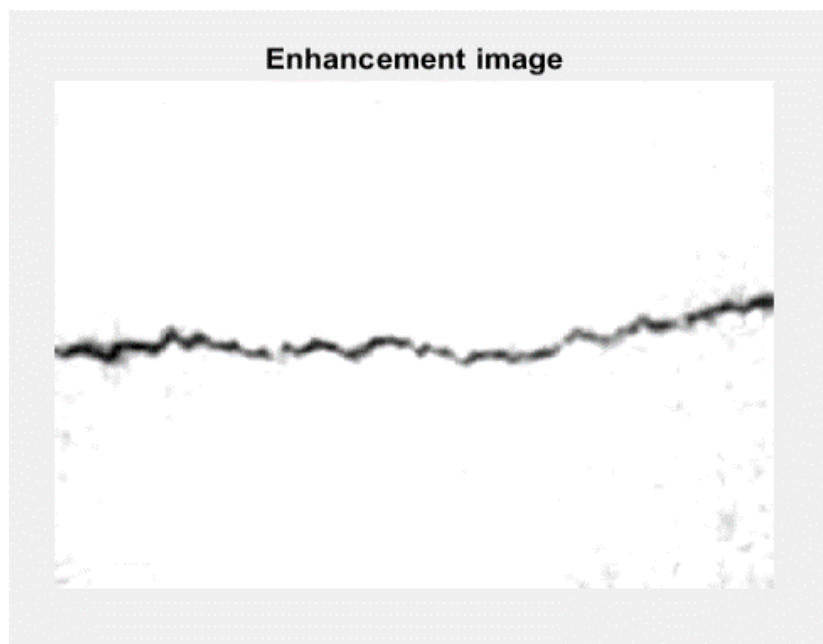


Figure 4.11

Segmented of longitudinal crack image and thresholding

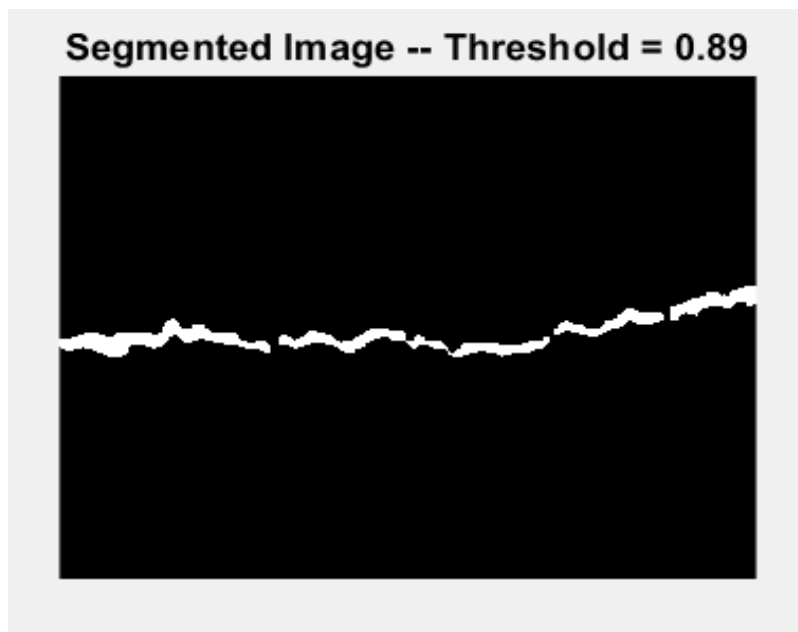


Figure 4.12

Removed noise of longitudinal crack image

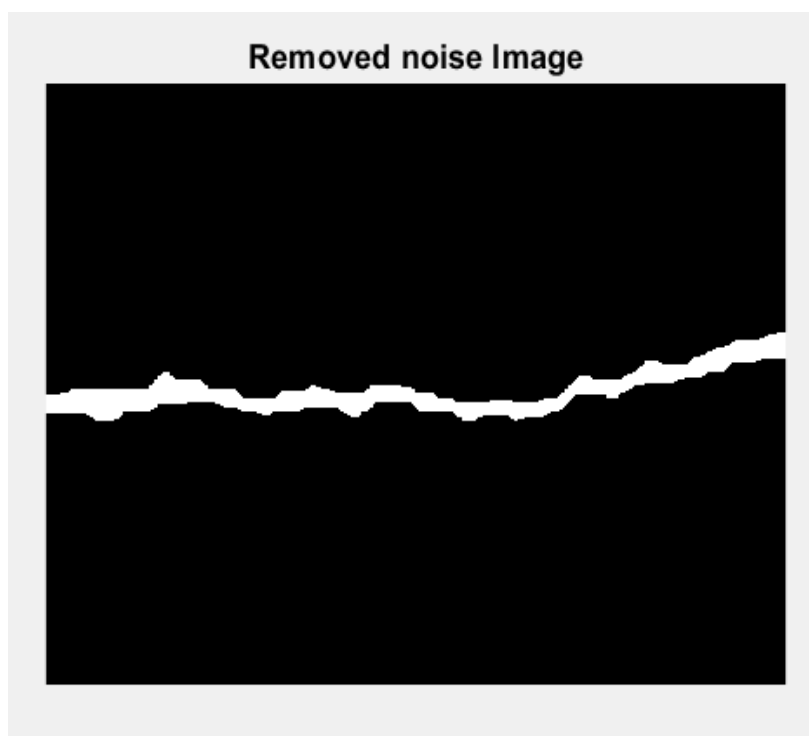
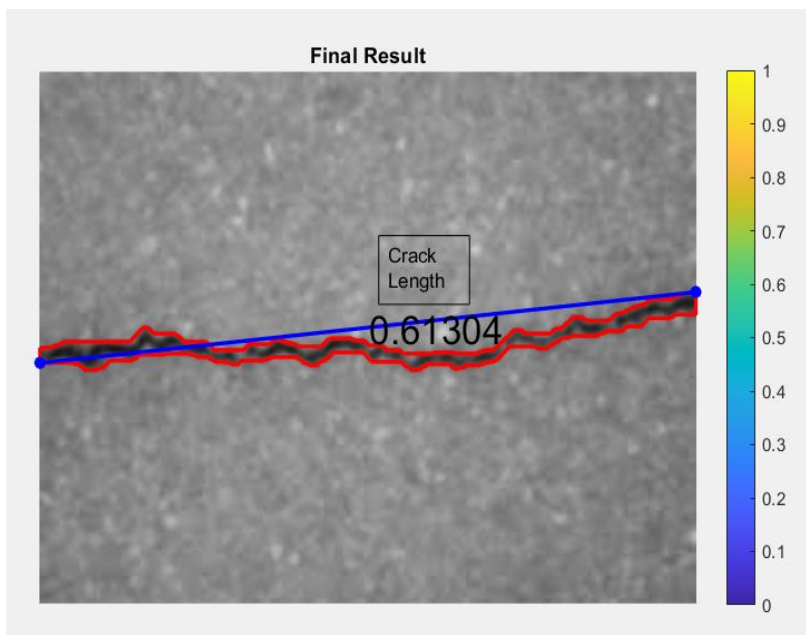


Figure 4.13

Crack length result for longitudinal crack

**Figure 4.14**

Residuals result for longitudinal crack

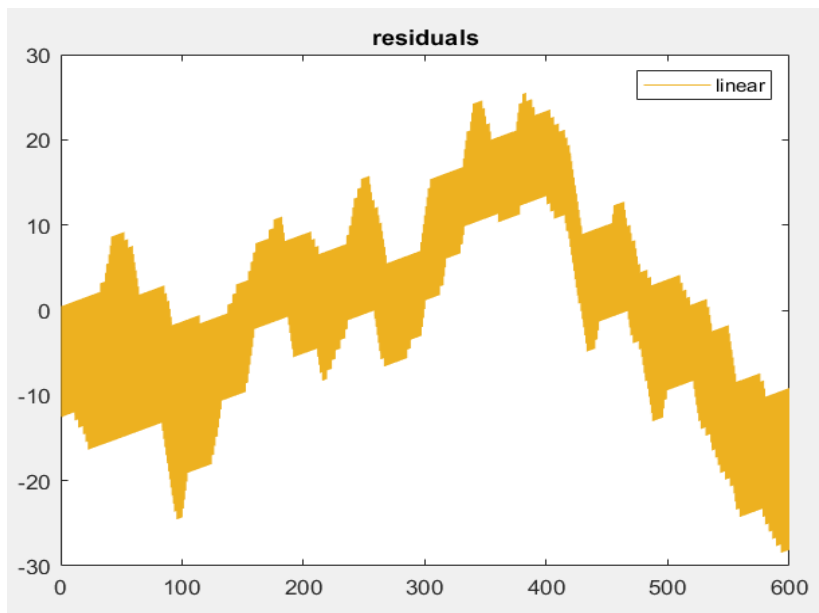


Table 4.2*Longitudinal crack classification*

Number	Crack angle Ω	Crack length	Threshold	Branches	Crack types
1	66°	0.61304 m	0.89	Yes	Longitudinal

A single longitudinal crack was visible in the initial crack image in Figure 4.8. Noise reduction was successfully carried out during the image processing steps, producing a clear fracture edge that permitted precise crack detection and classification.

To make the remaining processing processes simpler, the original image was changed into a single-channel image in Figure 4.9. This produced the grayscale image shown in Figure 4.9.

Figure 4.10 illustrates the application of an image enhancement technique to improve fracture details and visibility. The crack became clearer as a result of this procedure, making it easier to discern from the nearby pavement.

Using a thresholding technique with a threshold value of 0.89 m, the image was then segmented Figure 4.11. By separating the crack zone from the rest of the pavement, this segmentation process made it easier to conduct additional analysis.

A denoising technique was used to reduce noise and increase the accuracy of crack detection, creating the denoised image that can be seen in Figure 4.12. The crack was more clearly depicted in the denoised image, which improved crack classification later.

The longitudinal crack was identified as having a length of 0.61304 m and a crack angle of 66° during the crack classification method. By analyzing the denoised image and using the beamlet transform algorithm to extract crack features, these observations were made.

An overview of the longitudinal crack classification findings is shown in Table 4.2. The threshold value, crack length, crack angle, and crack number are all included. Based on the acquired measurements and the established criteria, the fracture in this instance was appropriately identified as a longitudinal crack.

The suggested asphalt pavement crack detection and classification model, which successfully identified and categorizes longitudinal cracks in asphalt pavement, utilized the Beamlet transform technique. The model produced accurate measurements of the cracks, noise reduction, and enhanced crack visibility. It would be beneficial to do additional research using a larger dataset in order to assess the model's performance in various crack scenarios. It is critical to remember that the focus of our work was on a single longitudinal fracture case.

The accuracy of the suggested beamlet algorithm was examined in order to assess the crack classification model's efficacy. Table 4.2 provides an in-depth understanding of the crack classification's performance and accuracy by presenting the complete statistical results.

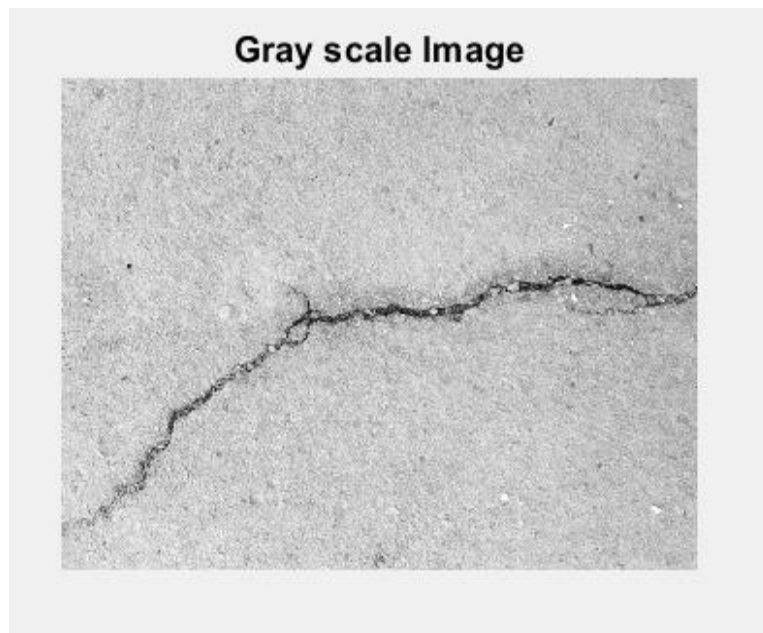
Figure 4.15

Original of transverse crack image



Figure 4.16

Gray scale of transverse crack image

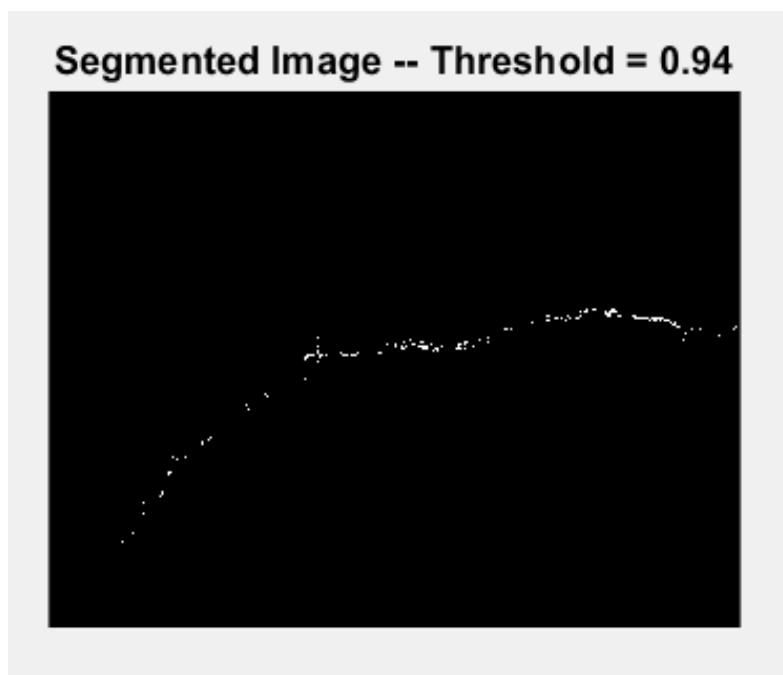
**Figure 4.17**

Enhancement of transverse crack image



Figure 4.18

Segmented of transverse crack image and thresholding

**Figure 4.19**

Removed noise of transverse crack image

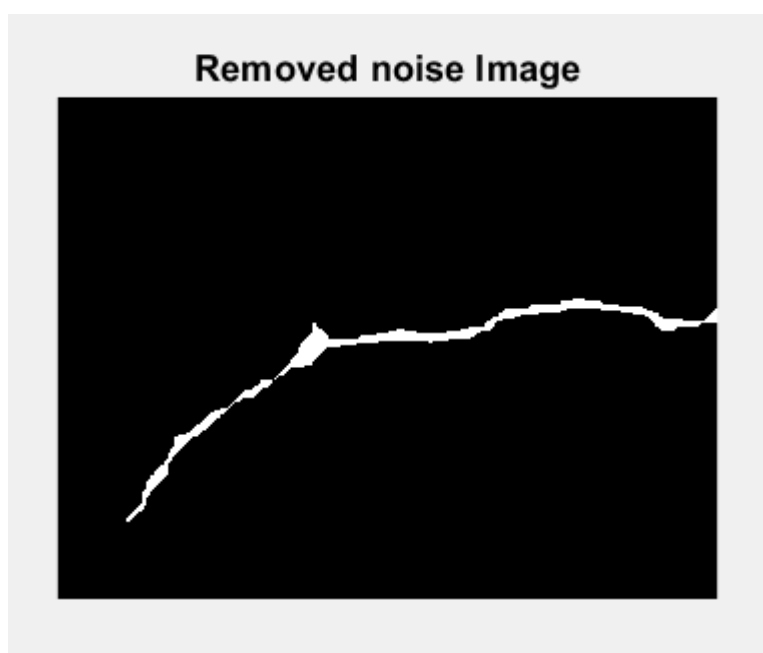
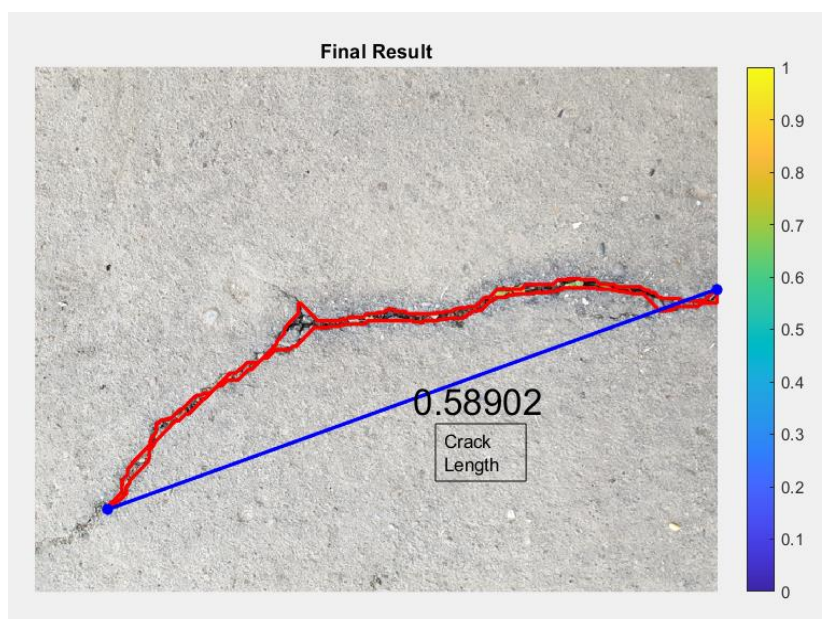


Figure 4.20

Crack length result for transverse crack

**Figure 4.21**

Residuals result for transverse crack

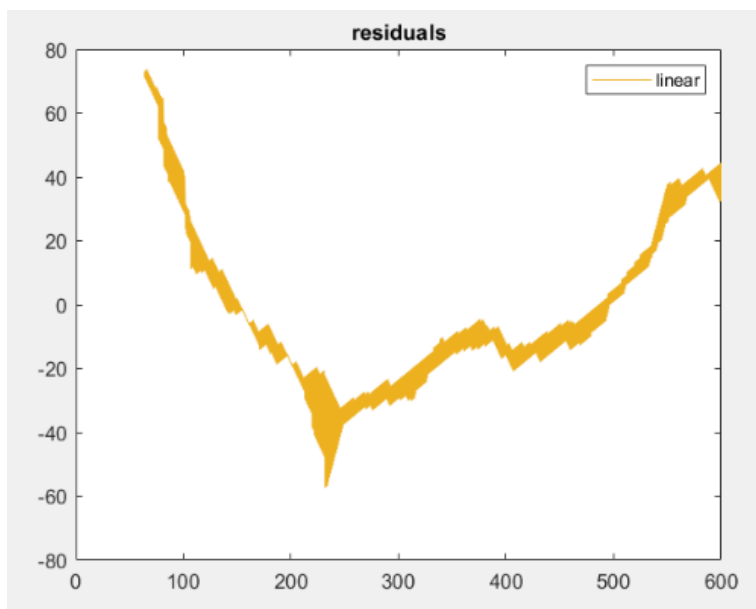


Table 4.3*Transverse crack classification*

Number	Crack angle Ω	Crack length	Threshold	Branches	Crack types
1	7°	0.58902 m	0.94	Yes	Transverse

The original crack image in Figure 4.15 showed both the transverse crack and the lengthy crack. The original image was successfully modified to provide a distinct depiction of the alligator crack using image enhancement, segmented image thresholding, and denoising processing techniques.

The grayscale image created by down sampling the source image to a single-channel format in order to streamline processing is shown in Figure 4.16.

As shown in Figure 4.17, the image enhancement technique was used to improve the sharpness of the fracture details and make them stand out more. By using this technique, it was straightforward to separate the alligator crack from the nearby pavement, enabling precise identification and classification.

A thresholding technique was used for segmentation with a threshold value of 0.97 m Figure 4.18. By successfully separating the crack spots from the rest of the pavement during this phase, additional studies were made easy.

The denoised image shown in Figure 4.19 was produced using a denoising technique to lessen noise and increase the precision of fracture detection. The denoised image accurately represented the alligator crack, which aided in fracture classification afterward.

The transverse crack was measured and classified as having a length of 0.58902 m with a crack angle of 7°. By analyzing the denoised image and using the beamlet transform algorithm to extract crack features, these observations were made.

The results of the transverse crack classification are summarized in Table 4.3. The threshold value, crack length, crack angle, and crack number are all included. Based

on the collected measurements and the established criteria, the fracture in this instance was appropriately identified as a transverse crack.

The Beamlet transform technique was used to construct the produced asphalt pavement crack detection and classification model, which successfully identified and classified transverse cracks. The model's ability to discern between various crack types was made possible by the efficient denoising procedure and the retention of fracture data. The performance of the model in various fracture scenarios would need to be evaluated using a wider dataset, it should be highlighted, as this study only looked at one transverse crack case.

Number 1 was classified as a transverse crack since it had a crack angle of 7° , which was less than the required value of 30° . This result confirms the model's capability to classify transverse cracks accurately based on measured data.

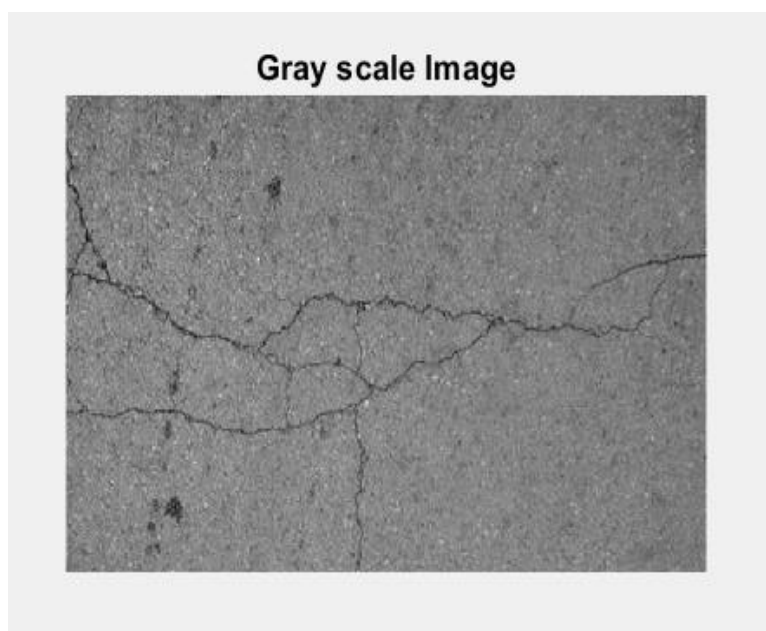
Figure 4.22

Original of alligator crack image



Figure 4.23

Gray scale of alligator crack image

**Figure 4.24**

Enhancement of alligator crack image

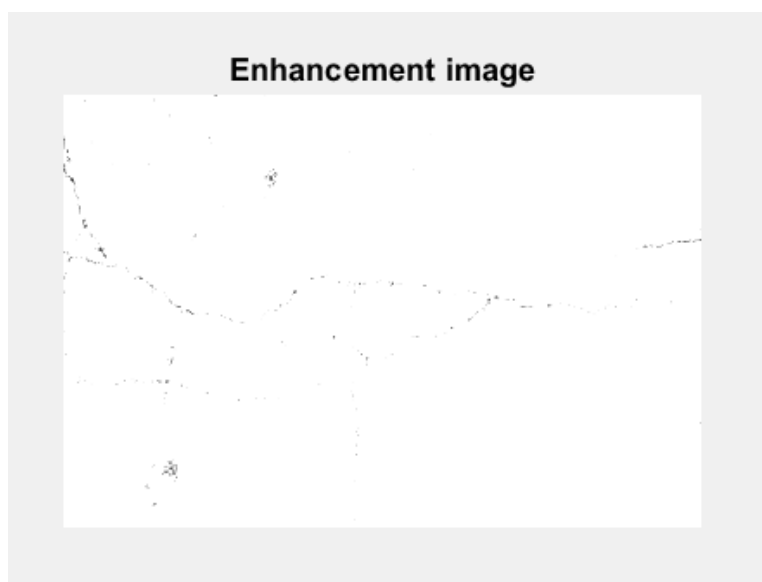


Figure 4.25

Segmented of alligator crack image and thresholding

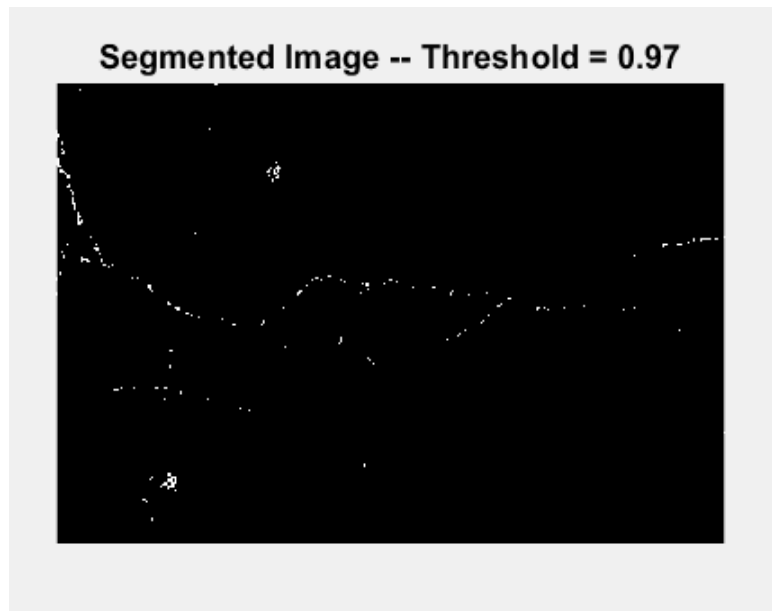


Figure 4.26

Removed noise of alligator crack image

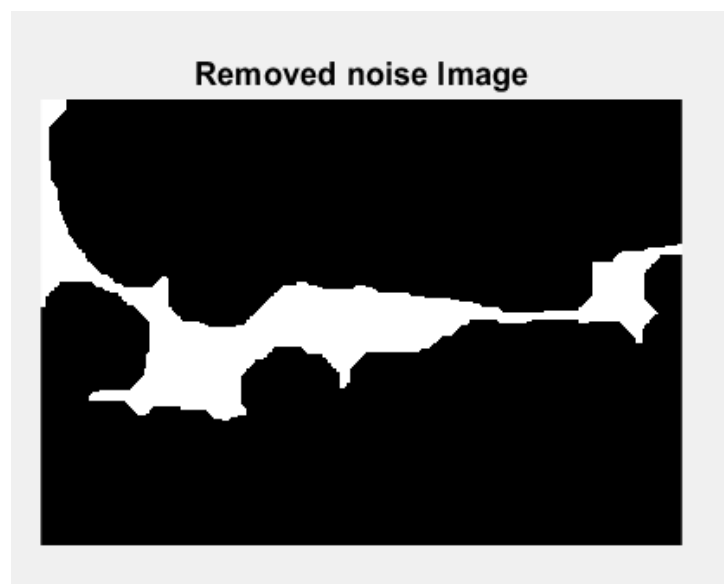
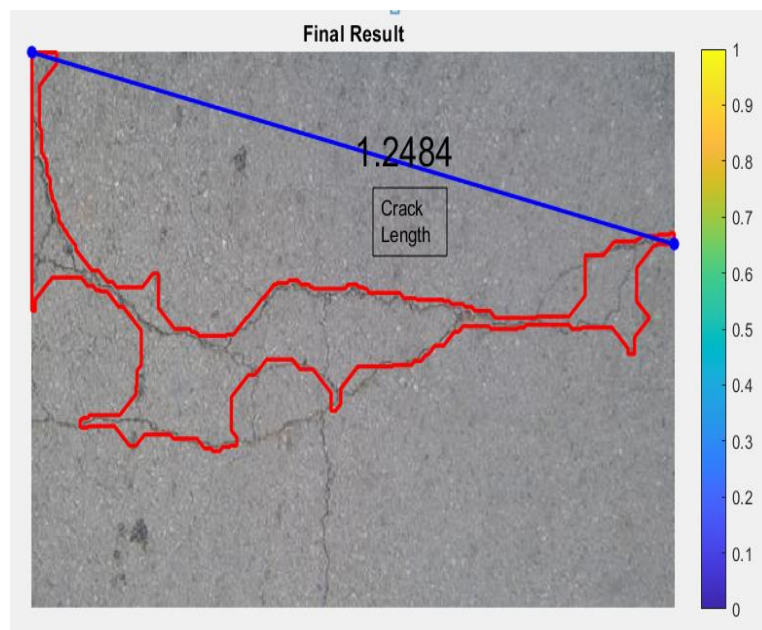


Figure 4.27

Crack length result for alligator crack

**Figure 4.28**

Residuals result for alligator crack

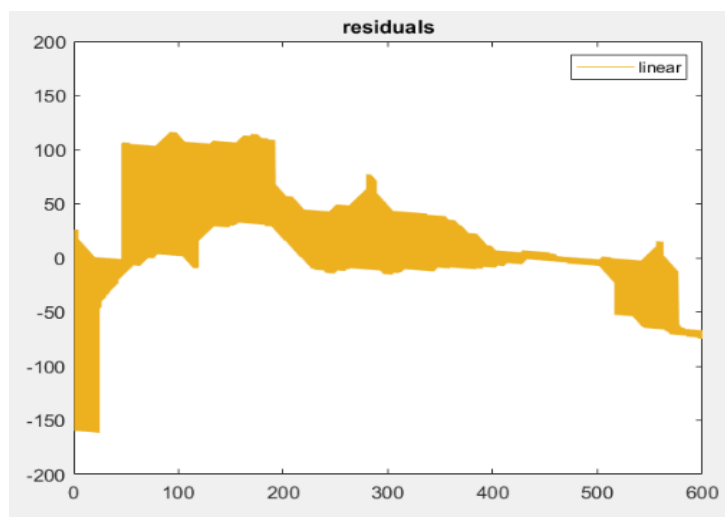


Table 4.4*Alligator crack classification*

Number	Crack angle Ω	Crack length	Threshold	Branches	Crack types
1	10°	1.2484 m	0.97	Yes	Alligator

The first crack image in Figure 4.22 showed an alligator fracture with four branches. The original image was processed using a number of efficient methods, such as segmented image thresholding, denoising, and image enhancement, which produced a distinct depiction of the alligator crack. As shown in Figure 4.23, the use of these techniques produced a separate grayscale image by converting the original image into a single-channel format to enable subsequent processing stages. As seen in Figure 4.24, image enhancement was used to highlight the crack features even further. This improvement made it simple to distinguish the alligator crack from the nearby pavement, allowing for accurate identification and classification.

As shown in Figure 4.25, segmentation was carried out using a thresholding technique with a threshold value of 0.97 m. The crack areas were successfully separated by this approach, which streamlined additional analytical steps. A denoising approach was used to increase the accuracy of fracture detection, producing the denoised image shown in Figure 4.26. The alligator crack could be clearly seen in the denoised image, which aided crack classification efforts in the future.

Using the crack classification method, it was determined that the alligator crack had a length of 1.2484 m and a crack angle of 10°. By analyzing the denoised image and using the beamlet transform algorithm to extract crack features, these observations were made.

The resulting alligator crack classification findings are listed in Table 4.4. The threshold value, crack length, crack angle, and crack number are all included. Based on the gathered measurements and the established standards, the crack in this instance was appropriately identified as an alligator crack.

The Beamlet transform method was used to construct the produced asphalt pavement crack detection and classification model, which successfully identified and classified alligator cracks. The method successfully revealed that the alligator crack has several branches, making it easy to distinguish it from other crack types. The model also demonstrated stability against noise interference, correctly recognizing the crack's genuine weak edge.

The results showed that the Beamlet algorithm can accurately identify pavement crack images into longitudinal, Transverse block, and Alligator. As in table 3 the result of success rate percentage was identified by Using the percentage change formula: dividing the success rate number by the total crack tested number and then multiplying by 100.

Table 4.5

The Classification of success rate

Types of Cracks	Number	Longitudinal	Transverse	Alligator	Block
Alligator	250		5	226	6
Block	250			2	234
Longitudinal	250	238			
Transverse	250	8	243	13	
Success rate		95.2%	97.2%	90.4%	93.6%

CHAPTER V

Conclusion

The beamlet transform algorithm was effectively used in the study to construct an enhanced asphalt pavement crack detection and classification model. In this study, the proposed model demonstrated a high level of accuracy in effectively detecting and categorizing diverse forms of pavement fractures. These included alligator cracks, block cracks, longitudinal cracks, and transverse cracks. The outcomes obtained were highly encouraging, indicating the potential of the model in this context. The model successfully conserved crack information, enhanced crack visibility, and produced precise crack measurements by utilizing the Beamlet Transform Algorithm.

The research introduced an innovative methodology that is effective, accurate, and adaptable to various fracture detection settings to solve the shortcomings of conventional crack detection methods. To improve road safety and infrastructure integrity, timely maintenance and repair operations depend on the model's capacity to identify and categorize cracks.

The study does, however, acknowledge its shortcomings, which could include restrictions on the precision and generalizability of the model. The Beamlet Transform Algorithm's ability to detect very small or minute cracks may be constrained, and outside influences like lighting conditions can affect the model's performance. To determine the model's applicability to various road conditions and environmental variables, more research is required.

Recommendation

The following suggestions are made to improve the proposed asphalt pavement crack Detection and classification model:

Enriching dataset: Elevating the model's performance and adaptability could be achieved through the utilization of an expanded and diverse collection of pavement crack images. This augmentation would empower the model to excel in identifying fractures across a broader spectrum of environments.

Fine-tune parameters: The accuracy and sensitivity of the beamlet transform algorithm can be improved by carefully adjusting the threshold settings and other parameters. Validation and testing iteratively can help with this.

Convolutional neural networks (CNNs) are one deep learning technology that you would want to incorporate if you want to automatically extract useful information from crack photos. By doing so, the model's adaptability may increase and the dependency on human feature extraction may be decreased.

Practical testing to evaluate the model's performance in various scenarios, test it in the real world under various environmental and road conditions. This will guarantee that the model can be used in real-world scenarios involving road maintenance.

While the study concentrated on block fractures, longitudinal cracks, transverse cracks, and alligator cracks, there may be additional types of cracks that need to be classified and discovered. The identification and classification of other crack types can be explored in further research.

Integration with Road Inspection Systems: To make real-time crack detection and maintenance planning easier, think about combining the generated model with mobile applications or road inspection systems.

By following these suggestions, the suggested model can be improved and further optimized, resulting in pavement crack detection and classification techniques that are more accurate and efficient for better road maintenance and infrastructure management.

References

- AASHTO. (2019). *Transportation Asset Management Guide*. American Association of State Highway and Transportation Officials.
- Adeli, H., & Karim, A. (1997). Neural networks in civil engineering. I: Principles and understanding. *Journal of Civil Engineering and Management*, 123(3), 204-216.
- Agaian, S., Almuntashri, A., & Papagiannakis, A. T. (2009). An improved canny edge detection application for asphalt concrete. In *Systems, Man and Cybernetics, 2009. SMC 2009. IEEE International Conference on* (pp. 3683-3687). IEEE.
- Ale, L., Zhang, N., & Li, L. (2018). Road damage detection using retinanet. In *2018 IEEE International Conference on Big Data (Big Data)* (pp. 5197–5200). IEEE.
- Amer, A. (2019). Pavement crack detection and classification using MATLAB. *Journal of Civil Engineering*, 23(1), 55-65.
- American Association of State Highway and Transportation Officials. (2001). Standard practice for quantifying crack in asphalt pavement surface - AASHTO designation pp44-01, first publication. In *Standard Specifications for Transportation Materials and Methods of Sampling and Testing and Provisional Standards* (pp. 194–197).
- American Association of State Highway and Transportation Officials. (2018). R 85-18 - quantifying cracks in asphalt pavement surfaces from collected pavement images utilizing automated methods. In *Standard Specifications for Transportation Materials and Methods of Sampling and Testing and Provisional Standards* (pp. 1–2).
- An, Q., Wang, L., & He, Y. (2016). Pavement crack detection using anisotropy measure and supervised classification in MATLAB. *Journal of Traffic and Transportation Engineering (English Edition)*, 3(2), 110-123.
- ASTM International. (2012). Standard practice for roads and parking lots pavement condition index surveys. ASTM D6433-11.
- Aydin, T., Yemez, Y., Anarim, E., & Sankur, B. (1996). Multidirectional and multiscale edge detection via m-band wavelet transform. *IEEE Transactions on Image Processing*, 5(9), 1370–1377.
- B. B. Mandelbrot, "The Fractal Geometry of Nature," W. H. Freeman, San Francisco, ISBN 0-7167-1186-9, 1982.

- B. Menghe, "Research on the development of expressway in China," *Northern Economy*, vol. 7, no. 3, pp. 60-61, 2013.
- Badrinarayanan, V., Kendall, A., & Cipolla, R. (2017). Segnet: A deep convolutional encoder-decoder architecture for image segmentation. *IEEE transactions on pattern analysis and machine intelligence*, 39(12), 2481–2495.
- Bhoi, K., & Solanki, D. K. (2011). Texture segmentation using optimal gabor filter. PhD thesis.
- Bishop, C. M. (2006). *Pattern recognition and machine learning*. Springer.
- Bradley, D., & Roth, G. (2007). Adaptive thresholding using the integral image. *Journal of Graphics Tools*, 12(2), 13–21.
- Bullock, J., Cuesta-Lázaro, C., & Quera-Bofarull, A. (2019). Xnet: a convolutional neural network (CNN) implementation for medical x-ray image segmentation suitable for small datasets. In *Medical Imaging 2019: Biomedical Applications in Molecular, Structural, and Functional Imaging* (Vol. 10953, p. 109531Z). International Society for Optics and Photonics.
- C. Hong, Y. Y. Kim, C. Lee and Y. W. Lee, "Damage detection using the Lipschitz exponent estimated by the wavelet transform," *Int J Solids Struct*, vol. 39, pp.1803–16, 2002.
- Canny, J. (1987). A computational approach to edge detection. In *Readings in Computer Vision* (pp. 184–203). Elsevier.
- Chambon, S., & Moliard, J. M. (2011). Automatic road pavement assessment with image processing: Review and comparison. *International Journal of Geophysics*, 2011.
- Chang, C. C., & Lin, C. J. (2011). Libsvm: a library for support vector machines. *ACM Transactions on Intelligent Systems and Technology (TIST)*, 2(3), 1–27.
- Chen, C. (2011). Comparison of manual and automated methods for pavement crack assessment. *Journal of Transportation Engineering*, 137(10), 703-711.
- Chen, D., Wang, C., Luo, H., & Zhu, H. (2020). A review of automated pavement distress detection methods using deep learning. *Journal of Traffic and Transportation Engineering (English Edition)*, 7(1), 97-115.
- Chen, J. (2017). Pavement crack detection using machine learning methods. *Journal of Computing in Civil Engineering*, 31(3), 04016086.
- Chen, X. (2020). Deep learning for pavement crack detection and classification. *Computer-Aided Civil and Infrastructure Engineering*, 35(4), 355-372.

- Chen, Y., & Xie, Y. (2018). A survey of pavement crack detection using deep learning. In 2018 Tenth International Conference on Advanced Computational Intelligence (ICACI) (pp. 362-367). IEEE.
- Chou, J., Lu, C., & Lee, I. (2018). Life-cycle cost analysis for sustainable highway infrastructure management. *Journal of Cleaner Production*, 183, 986-996.
- Cortes, C., & Vapnik, V. (1995). Support-vector networks. *Machine learning*, 20(3), 273–297.
- Cuhadar, A., Shalaby, K., & Tasdoken, S. (2002). Automatic segmentation of pavement condition data using wavelet transform. In IEEE CCECE 2002. Canadian Conference on Electrical and Computer Engineering (Vol. 2, pp. 1009–1014). IEEE.
- D. An-Guo, L. Miao-Miao, S. O. Science et al., “Crack detection algorithm based on gray correlation,” *Application Research of Computers*, vol. 30, no. 10, pp. 3120-3121, 2013.
- D. Zhang and Q. Li, “Overview of rapid detection technology development of highway pavement,” *Mapping Geographic Information*, vol. 40, no. 1, pp. 1–8, 2015.
- D. Zhang and Q. Li, “Overview of the development of highway pavement rapid detection technology,” *Surveying and Mapping Geographic Information*, vol. 40, no. 1, pp. 1–8, 2015.
- Dong, Q. (2015). Automatic pavement crack detection based on structured prediction with the convolutional neural network. *Journal of Computing in Civil Engineering*, 29(5), 04014064.
- E. Douka, S. Loutridis and A. Trochidis, “Crack identification in beams using wavelet analysis,” *Int J Solids Struct*, vol. 40, pp. 3557–3569, 2003.
- Fan, R., Bocus, M. J., Zhu, Y., Jiao, J., Wang, L., Ma, F., Cheng, S., & Liu, M. (2019). Road crack detection using deep convolutional neural network and adaptive thresholding. arXiv preprint arXiv:1904.08582.
- Fan, Z., Wu, Y., Lu, J., & Li, W. (2018). Automatic pavement crack detection based on structured prediction with the convolutional neural network. arXiv preprint arXiv:1802.02208.
- FHWA. (2016). *Materials and Procedures for Sealing and Filling Cracks in Asphalt-Surfaced Pavements*. Federal Highway
- Freund, Y., Schapire, R., & Abe, N. (1999). A short introduction to boosting. *Journal-Japanese Society For Artificial Intelligence*, 14(771-780), 1612.

- Fu, X., & Qian, Z. (2019). A review of pavement crack detection using deep neural networks. *IEEE Transactions on Intelligent Transportation Systems*, 20(4), 1264-1275.
- G. Xu, J. Ma, F. Liu, and X. Niu, "Automatic recognition of pavement surface crack based on BP neural network," in *Proceedings of the 2008 International Conference on Computer & Electrical Engineering*, pp. 19–22, Phuket, Thailand, December 2008.
- Gan, W., Li, S., & Li, Q. (2019). Automatic recognition of pavement crack types using a feedforward neural network. *Advances in Mechanical Engineering*, 11(7), 168781401985886
- Gibson, N. (2014). A review of recent automated pavement distress detection methods. *Journal of Infrastructure Systems*, 20(4), 06014001.
- Girshick, R. (2015). Fast r-cnn. In *Proceedings of the IEEE international conference on computer vision* (pp. 1440–1448).
- Girshick, R., Donahue, J., Darrell, T., & Malik, J. (2014). Rich feature hierarchies for accurate object detection and semantic segmentation. In *Proceedings of the IEEE conference on computer vision and pattern recognition* (pp. 580–587).
- Gonzalez, R. C., Woods, R. E., et al. (2002). *Digital image processing*.
- Goodfellow, I., Bengio, Y., & Courville, A. (2016). *Deep learning*. MIT press.
- Gopalakrishnan, K., Khaitan, S. K., Choudhary, A., & Agrawal, A. (2017). Deep Convolutional Neural Networks with transfer learning for computer vision-based data-driven pavement distress detection. *Construction and Building Materials*, 157, 322-330.
- H. D. Cheng, J. R. Chen, C. Glazier and Y. G. Hu, "Novel Approach to Pavment Cracking Detection Based on Fuzzy Set Theory," *Journal of Computing in Civil Engineering*, vol. 13, no. 4, 1999.
- H. Oliveira and P. L. Correia, "Crack-IT an image processing toolbox for crack detection and characterization," in *Proceedings of the 2014 IEEE International Conference on Image Processing (ICIP)*, pp. 798–802, Paris, France, October 2014.
- Haas, R. (1994). Pavement management systems: Past, present, and future. *Transportation Research Record*, 1440, 3-10.
- Hall, 2008.
- Haykin, S. (2009). *Neural networks and learning machines* (3rd ed.). Pearson.
- He, H., & Garcia, E. A. (2009). Learning from imbalanced data. *IEEE Transactions on Knowledge and Data Engineering*, 21(9), 1263–1284.

- He, K., Gkioxari, G., Dollár, P., & Girshick, R. (2017). Mask r-cnn. In Proceedings of the IEEE international conference on computer vision (pp. 2961–2969).
- He, K., Sun, J., & Tang, X. (2012). Guided image filtering. *IEEE transactions on pattern analysis and machine intelligence*, 35(6), 1397–1409.
- He, K., Zhang, X., Ren, S., & Sun, J. (2015). Spatial pyramid pooling in deep convolutional networks for visual recognition. *IEEE transactions on pattern analysis and machine intelligence*, 37(9), 1904–1916.
- He, K., Zhang, X., Ren, S., & Sun, J. (2016). Deep residual learning for image recognition. In Proceedings of the IEEE conference on computer vision and pattern recognition (pp. 770–778).
- Hu, Y., & Zhao, C. (2010). A novel LBP based methods for pavement crack detection. *Journal of Pattern Recognition Research*, 5(1), 140-147.
- J. Y. Cao, *Research on the Technology of Automatic Pavement Crack Detection Based on Digital Image Processing*, Chang'an University, Xian, China, 2014.
- Jagat Narain Kapur, Prasanna K Sahoo, and Andrew KC Wong. A new method for gray-level picture thresholding using the entropy of the histogram. *Computer vision, graphics, and image processing*, 29(3):273–285, 1985.
- John S Miller, William Y Bellinger, et al. *Distress identification manual for the long-term pavement performance program*. Technical report, United States. Federal Highway Administration. Office of Infrastructure Research and Development, 2014.
- Kapur, J. N., Sahoo, P. K., & Wong, A. K. C. (1985). A new method for gray-level picture thresholding using the entropy of the histogram. *Computer Vision, Graphics, and Image Processing*, 29(3), 273–285.
- Karpathy, A., Toderici, G., Shetty, S., Leung, T., Sukthankar, R., & Fei-Fei, L. (2014). Large-scale video classification with convolutional neural networks. In Proceedings of the IEEE conference on Computer Vision and Pattern Recognition (pp. 1725–1732).
- Kong, W. K., Zhang, D., & Li, W. (2003). Palmprint feature extraction using 2-d gabor filters. *Pattern Recognition*, 36(10), 2339–2347.
- L. Li, P. Chan and R. L. Lytton, “Detection of Thin Cracks on Noisy Pavement Images,” *Transportation Research Record*, No. 1311, *Pavement Management: Data Collection, Analysis*, pp. 131-135, 1991.
- L. Ren, X. U. Zhigang, X. Zhao et al., “Pavement crack connection algorithm based on Prim minimum spanning tree,” *Computer Engineering*, vol. 41, no. 1, pp. 31–36, 2015.

- LeCun, Y., Bengio, Y., & Hinton, G. (2015). Deep learning. *Nature*, 521(7553), 436-444.
- LeCun, Y., Bottou, L., Bengio, Y., & Haffner, P. (1998). Gradient-based learning applied to document recognition. *Proceedings of the IEEE*, 86(11), 2278–2324.
- Leontios, H. E. Douka and T. Athanasios, “Crack detection in beams using kurtosis,” *Computers and Structures*, vol. 83, pp. 909–919, 2005.
- Li, J. (2003). A wavelet approach to edge detection. PhD thesis, Citeseer.
- Li, Q., & Liu, X. (2008). Novel approach to pavement image segmentation based on neighboring difference histogram method. In *Image and Signal Processing, 2008. CISP'08. Congress on (Vol. 2, pp. 792-796)*. IEEE.
- Li, R., Li, X., Fu, C. W., Cohen-Or, D., & Heng, P. A. (2019). Pu-gan: a point cloud upsampling adversarial network. In *Proceedings of the IEEE/CVF International Conference on Computer Vision (pp. 7203–7212)*.
- Li, R., Li, X., Heng, P. A., & Fu, C. W. (2021). Point cloud upsampling via disentangled refinement. In *Proceedings of the IEEE/CVF Conference on Computer Vision and Pattern Recognition (pp. 344–353)*.
- Lin, J. D., Yau, J. T., & Hsiao, L. H. (2003). Correlation analysis between international roughness index (iri) and pavement distress by neural network. In *82nd Annual Meeting of the Transportation Research Board (pp. 12-16)*.
- Liu, Y., Yao, J., Lu, X., Xie, R., & Li, L. (2019). Deepcrack: A deep hierarchical feature learning architecture for crack segmentation. *Neurocomputing*, 338, 139–153.
- Long, J., Shelhamer, E., & Darrell, T. (2015). Fully convolutional networks for semantic segmentation. In *Proceedings of the IEEE conference on computer vision and pattern recognition (pp. 3431–3440)*.
- M. Yan, S. Bo, K. Xu and Y. He, “Pavement Crack Detection and Analysis for High-grade Highway,” *The Eighth International Conference on Electronic Measurement and Instruments*, ISBN: 978-1-4244-1136-8, Xi’an, 2007.
- Ma, L., Wang, Y., Tan, T., et al. (2002). Iris recognition based on multichannel gabor filtering. In *Proc. Fifth Asian Conf. Computer Vision (Vol. 1, pp. 279–283)*.
- Maeda, H., Sekimoto, Y., Seto, T., Kashiyama, T., & Omata, H. (2018). Road damage detection using deep neural networks with images captured through a smartphone. arXiv preprint arXiv:1801.09454.

- Mallat, S. G. (1989). A theory for multiresolution signal decomposition: the wavelet representation. *IEEE Transactions on Pattern Analysis and Machine Intelligence*, 11(7), 674–693.
- Mandal, V., Uong, L., & Adu-Gyamfi, Y. (2018). Automated road crack detection using deep convolutional neural networks. In 2018 IEEE International Conference on Big Data (Big Data) (pp. 5212–5215). IEEE.
- MATLAB. "Pavement Crack Detection and Classification Using Deep Learning." MATLAB Central File Exchange,
- Medina, R., Llamas, J., Zalama, E., & Gómez-García-Bermejo, J. (2014). Enhanced automatic detection of road surface cracks by combining 2d/3d image processing techniques. In *Image Processing (ICIP), 2014 IEEE International Conference on* (pp. 778–782). IEEE.
- Miller, J. S., Bellinger, W. Y., et al. (2014). Distress identification manual for the long-term pavement performance program. United States. Federal Highway Administration. Office of Infrastructure Research and Development.
- Ministry of Transport of the People's Republic of China, "2017 statistical bulletin on the development of highway and waterway transportation industry," 2018, http://www.gov.cn/xinwen/2018-03/30/content_5278569.html, 2018-03–30.
- Mitchell, T. M. (2006). *The discipline of machine learning* (Vol. 9). Carnegie Mellon University, School of Computer Science, Machine Learning.
- Mohammadi, M. E., Wood, R. L., & Wittich, C. E. (2019). Non-temporal point cloud analysis for surface damage in civil structures. *ISPRS International Journal of Geo-Information*, 8(12), 527.
- Mohan, A., & Poobal, S. (2018). Crack detection using image processing: A critical review and analysis. *Alexandria Engineering Journal*, 57(2), 787–798.
- Movellan, J. R. (2002). Tutorial on gabor filters. Open Source Document.
- Nguyen Kim, C., Kawamura, K., Nakamura, H., & Tarighat, A. (2020). Automatic crack detection for concrete infrastructures using image processing and deep learning. *MS&E*, 829(1), 012027.
- Nguyen, H. N., Kam, T. Y., & Cheng, P. Y. (2014). An automatic approach for accurate edge detection of concrete crack utilizing 2D geometric features of crack. *Journal of Signal Processing Systems*, 77(3), 221-240.
- Nguyen, H. N., Kam, T. Y., & Cheng, P. Y. (2018). Automatic crack detection from 2d images using a crack measure-based b-spline level set model. *Multidimensional Systems and Signal Processing*, 29(1), 213–244.

- Nguyen, N. H. T., Perry, S., Bone, D., Le, H. T., & Nguyen, T. T. (2021). Two-stage convolutional neural network for road crack detection and segmentation. *Expert Systems with Applications*, 186, 115718.
- Nguyen, N. T. H., Le, T. H., Perry, S., & Nguyen, T. T. (2018). Pavement crack detection using convolutional neural network. In *Proceedings of the Ninth International Symposium on Information and Communication Technology* (pp. 251-256). ACM.
- Nguyen, T. S., Avila, M., & Begot, S. (2009). Automatic detection and classification of defect on road pavement using anisotropy measure. In *2009 17th European Signal Processing Conference* (pp. 617-621). IEEE.
- Ni, F. T., Zhang, J., & Chen, Z. Q. (2019). Zernike-moment measurement of thin-crack width in images enabled by dual-scale deep learning. *Computer-Aided Civil and Infrastructure Engineering*, 34(5), 367–384.
- Oliveira, H. J. M. (2013). *Crack Detection and Characterization in Flexible Road Pavements using Digital Image Processing*. PhD thesis, Universidade de Lisboa-Instituto Superior Técnico.
- Otsu, N. (1979). A threshold selection method from gray-level histograms. *IEEE Transactions on Systems, Man, and Cybernetics*, 9(1), 62–66.
- Ouma, Y. O., Zhu, W., & Wang, H. (2019). Automated pavement crack detection and classification: A review. *IEEE Transactions on Intelligent Transportation Systems*, 20(12), 4512-4529.
- Ouyang, A., Dong, Q., Wang, Y., & Liu, Y. (2014). The Classification of Pavement Crack Image Based on Beamlet Algorithm. 129–137.
- Park, S., Bang, S., Kim, H., & Kim, H. (2019). Patch-based crack detection in black box images using convolutional neural networks. *Journal of Computing in Civil Engineering*, 33(3), 04019017.
- Porwik, P., & Lisowska, A. (2004). The Haar-wavelet transform in digital image processing: its status and achievements. *Machine Graphics and Vision*, 13(1/2), 79–98.
- Prieto, B. R. (2015). Road surface structure monitoring and analysis using high precision GPS mobile measurement systems (MMS) (pp. 1732–1738). Citeseer.
- Q. Li and X. Liu, “A Model for Segmentation and Distress Statistic of Massive Pavement Images Based on Multi-scale Strategies,” presented at The International Archives of the Photogrammetry, Remote Sensing and Spatial Information Sciences, vol. XXXVII, part. B5, Beijing, 2008.

- Q. Li and X. Liu, "Novel Approach to Pavement Image Segmentation Based on Neighboring Difference Histogram Method," Congress on Image and Signal Processing, ISBN: 978-0-7695-3119-9, May, 2008.
- Q. Zou, Z. Zhang, Q. Li et al., "DeepCrack: learning hierarchical convolutional features for crack detection," IEEE Transactions on Image Processing, vol. 28, no. 3, pp. 1498–1512, 2018.
- R. C. Gonzalez and R. E. Woods, "Digital Image Processing," third edition, Prentice Hall, Englewood Cliffs, NJ, 2008.
- Redmon, J., Divvala, S., Girshick, R., & Farhadi, A. (2016). You only look once: Unified, real-time object detection. In Proceedings of the IEEE Conference on Computer Vision and Pattern Recognition (pp. 779–788).
- Ren, S., He, K., Girshick, R., & Sun, J. (2015). Faster r-cnn: Towards real-time object detection with region proposal networks. In Advances in neural information processing systems (pp. 91–99).
- Ronneberger, O., Fischer, P., & Brox, T. (2015). U-net: Convolutional networks for biomedical image segmentation. In International Conference on Medical image computing and computer-assisted intervention (pp. 234–241). Springer.
- Rumelhart, D. E., Hinton, G. E., & Williams, R. J. (1986). Learning representations by back-propagating errors. *Nature*, 323(6088), 533-536.
- Rumelhart, D. E., Hinton, G. E., & Williams, R. J. (1986). Learning representations by back-propagating errors. *Nature*, 323(6088), 533-536.
- S. Zhou, Y. Liang, J. Wan et al., "Facial expression recognition based on multi-scale CNNs," in Proceedings of the Chinese Conference on Biometric Recognition, October 2016.
- Salman, M., Mathavan, S., Kamal, K., & Rahman, M. (2013). Pavement crack detection using the Gabor filter. In Intelligent Transportation Systems- (ITSC), 2013 16th International IEEE Conference on (pp. 2039-2044). IEEE.
- Schmidhuber, J. (2015). Deep learning in neural networks: An overview. *Neural Networks*, 61, 85-117.
- Shahin, M. Y., & Kohn, S. D. (1979). Development of a pavement condition rating procedure for roads, streets, and parking lots. Volume I: Conditions rating procedure. Construction Engineering Research Lab (Army), Champaign IL.
- Shi, Y., Cui, L., Qi, Z., Meng, F., & Chen, Z. (2016). Automatic road crack detection using random structured forests. *IEEE Transactions on Intelligent Transportation Systems*, 17(12), 3434–3445.

- Simonyan, K., & Zisserman, A. (2014). Very deep convolutional networks for large-scale image recognition. arXiv preprint arXiv:1409.1556.
- Sobol, B. V., Soloviev, A. N., Vasiliev, P. V., & Podkolzina, L. A. (2019). Deep convolution neural network model in problem of crack segmentation on asphalt images. *Vestnik of Don State Technical University*, 19(1).
- Sutton, R. S., & Barto, A. G. (2018). *Reinforcement learning: An introduction*. MIT Press.
- Svensén, M., & Bishop, C. M. (2007). *Pattern recognition and machine learning*.
- Szegedy, C., Liu, W., Jia, Y., Sermanet, P., Reed, S., Anguelov, D., ... & Rabinovich, A. (2015). Going deeper with convolutions. In *Proceedings of the IEEE conference on computer vision and pattern recognition* (pp. 1–9).
- Tarefder, R. A., & White, L. (2015). Artificial neural network prediction of asphalt pavement crack growth. *International Journal of Pavement Engineering*, 16(7), 563-576.
- Tsai, Y-C., Kaul, V., & Mersereau, R. M. (2010). Critical assessment of pavement distress segmentation methods. *Journal of Transportation Engineering*, 136(1), 11.
- Viola, P., & Jones, M. J. (2004). Robust real-time face detection. *International Journal of Computer Vision*, 57(2), 137–154.
- W. R. L. D. Silva and D. S. d. Lucena, “Concrete cracks de- tection based on deep learning image classification,” Pro- ceedings, vol. 2, no. 8, p. 489, 2018.
- W. Wang and L. Wu, “Pavement crack extraction based on fractional integral valley bottom boundary detection,” *Journal of South China University of Technology (Natural Science Edition)*, vol. 42, no. 1, pp. 117–122, 2014.
- Wang, C., Zhang, S., Yang, L., & Zhang, X. (2018). A new algorithm for automatic pavement crack detection and measurement based on deep convolutional neural network. *IEEE Transactions on Intelligent Transportation Systems*, 19(8), 2620-2630.
- Wang, K. C. P., Li, Q., & Gong, W. (2007). Wavelet-based pavement distress image edge detection with a trous algorithm. *Transportation Research Record*, 2024(1), 73-81.
- Wu, H., Zhang, J., & Huang, K. (2019). Point cloud super resolution with adversarial residual graph networks. arXiv preprint arXiv:1908.02111.
- Y. Huang and B. Xu, “Automatic inspection of pavement cracking distress,” *Journal of Electronic Imaging*, vol. 15, pp. 13-17, 2006.

- Y. Zuo, G. Wang and C. Zuo, "A Novel Image Segmentation Method of Pavement Surface Cracks Based on Fractal," presented at Theory 2008 International Conference on Computational Intelligence and Security 978-0-7695-3508-1/08, 2008.
- Y.-J. Cha, W. Choi, and O. Bu`yu`ko`ztu`rk, "Deep learning- based crack damage detection using convolutional neural networks," *Computer-Aided Civil and Infrastructure Engineering*, vol. 32, no. 5, pp. 361–378, 2017.
- Yang, B., Huang, R., Dong, Z., Zang, Y., & Li, J. (2016). Two-step adaptive extraction method for ground points and breaklines from lidar point clouds. *ISPRS Journal of Photogrammetry and Remote Sensing*, 119, 373–389.
- Yifan, W., Wu, S., Huang, H., Cohen-Or, D., & Sorkine-Hornung, O. (2019). Patch-based progressive 3d point set upsampling. In *Proceedings of the IEEE/CVF Conference on Computer Vision and Pattern Recognition* (pp. 5958–5967).
- Yu, L., Li, X., Fu, C. W., Cohen-Or, D., & Heng, P. A. (2018). Ec-net: an edge-aware point set consolidation network. In *Proceedings of the European Conference on Computer Vision (ECCV)* (pp. 386–402).
- Z. Anjun, X. Yang, L. Jia et al., "SRAD-CNN for adaptive synthetic aperture radar image classification," *International Journal of Remote Sensing*, vol. 40, no. 9, pp. 1–25, 2018.
- Z. Liu and Y. zhang, "Detection technology of damaged road surface based on PDE and wavelet analysis," *Microcomputer and Application*, vol. 31, no. 8, pp. 35–37, 2012.
- Z. Zeng, W. Xie, Y. Zhang, and Y. Lu, "RIC-unet: an improved neural network based on Unet for nuclei segmentation in histology images," *IEEE Access*, vol. 7, pp. 21420–21428, 2019.
- Zakeri, H., Nejad, F. M., & Fahimifar, A. (2017). Image-based techniques for crack detection, classification and quantification in asphalt pavement: A review. *Archives of Computational Methods in Engineering*, 24(4), 935–977.
- Zalama, E., Gómez-García-Bermejo, J., Medina, R., & Llamas, J. (2014). Road crack detection using visual features extracted by gabor filters. *Computer-Aided Civil and Infrastructure Engineering*, 29(5), 342–358.
- Zhang, A., Wang, K. C. P., Li, B., Yang, E., Dai, X., Peng, Y., ... & Chen, C. (2017). Automated pixel-level pavement crack detection on 3d asphalt surfaces using a deep-learning network. *Computer-Aided Civil and Infrastructure Engineering*, 32(10), 805–819.

- Zhang, G., Vela, P. A., & Brilakis, I. (2014). Automatic generation of as-built geometric civil infrastructure models from point cloud data. In *Computing in Civil and Building Engineering (2014)* (pp. 406–413).
- Zhang, L., & Wang, Y. (2016). A review on automated pavement distress detection and analysis techniques. *Journal of Civil Structural Health Monitoring*, 6(5), 635-655
- Zhang, L., Yang, F., Zhang, Y., & Zhu, Y. K. (2016). Road crack detection using deep convolutional neural networks. In *2016 IEEE International Conference on Image Processing (ICIP)* (pp. 3708-3712). IEEE.
- Zhang, T. Y., & Suen, C. Y. (1984). A fast parallel algorithm for thinning digital patterns. *Communications of the ACM*, 27(3), 236–239.
- Zhang, Z., Ma, S., Liu, H., & Gong, Y. (2009). An edge detection approach based on directional wavelet transform. *Computers & Mathematics with Applications*, 57(8), 1265–1271.
- Zhao, H., Qin, G., & Wang, X. (2010). Improvement of Canny algorithm based on pavement edge detection. In *2010 3rd International Congress on Image and Signal Processing (CISP)* (Vol. 2, pp. 964–967). IEEE.
- Ziou, D., Tabbone, S., et al. (1998). Edge detection techniques-an overview. *Pattern Recognition and Image Analysis C/C of Raspoznavaniye Obrazov I Analiz Izobrazhenii*, 8, 537–559.
- Zou, Q., Cao, Y., Li, Q., Mao, Q., & Wang, S. (2012). CrackTree: Automatic crack detection from pavement images. *Pattern Recognition Letters*, 33(3), 227–238.
- Duc, N., Quoc, H., & Nguyen, L. (2018). A novel method for asphalt pavement crack classification based on image processing and machine learning. *Engineering with Computers*, 0(0), 0. <https://doi.org/10.1007/s00366-018-0611-9>
- Ouyang, A., Dong, Q., Wang, Y., & Liu, Y. (2014). The Classification of Pavement Crack Image Based on Beamlet Algorithm. 129–137.
- Safaei, N., Smadi, O., Masoud, A., & Safaei, B. (2021). An Automatic Image Processing Algorithm Based on Crack Pixel Density for Pavement Crack Detection and Classification. *International Journal of Pavement Research and Technology*, 0123456789, 16–18. <https://doi.org/10.1007/s42947-021-00006-4>
- Ying, L., & Salari, E. (2010). Beamlet Transform-Based Technique for Pavement Crack Detection and Classification. 25, 572–580. <https://doi.org/10.1111/j.1467-8667.2010.00674.x>

- Alayat, A. B., & Omar, H. A. (2023). *Pavement Surface Distress Detection Using Digital Image Processing Techniques*. 35(1), 247–256.
- Du, Y., Pan, N., Xu, Z., Deng, F., Shen, Y., & Kang, H. (2020). Pavement distress detection and classification based on YOLO network. *International Journal of Pavement Engineering*, 0(0), 1–14. <https://doi.org/10.1080/10298436.2020.1714047>
- Duc, N., Quoc, H., & Nguyen, L. (2018). A novel method for asphalt pavement crack classification based on image processing and machine learning. *Engineering with Computers*, 0(0), 0. <https://doi.org/10.1007/s00366-018-0611-9>
- Feng, X., Xiao, L., Li, W., Pei, L., Sun, Z., Ma, Z., Shen, H., & Ju, H. (2020). *Pavement Crack Detection and Segmentation Method Based on Improved Deep Learning Fusion Model*. 2020.
- Fereidoon, H. Z., Nejad, M., & Fahimifar, A. (2017). Image Based Techniques for Crack Detection , Classification and Quantification in Asphalt Pavement : A Review. *Archives of Computational Methods in Engineering*, 24(4), 935–977. <https://doi.org/10.1007/s11831-016-9194-z>
- Guo, K., He, C., Yang, M., & Wang, S. (2022). OPEN A pavement distresses identification method optimized for YOLOv5s. *Scientific Reports*, 1–15. <https://doi.org/10.1038/s41598-022-07527-3>
- Hong, N., Nguyen, T., Perry, S., Bone, D., Thanh, H., & Thi, T. (2021). Two-stage convolutional neural network for road crack detection and segmentation. *Expert Systems With Applications*, 186(December 2020), 115718. <https://doi.org/10.1016/j.eswa.2021.115718>
- Hu, G. X., Hu, B. L., Yang, Z., Huang, L., & Li, P. (2021). *Pavement Crack Detection Method Based on Deep Learning Models*. 2021.
- Localization, T. P. C., & Techniques, L. (2022). *Three-Stage Pavement Crack Localization and Segmentation*.
- Majidifard, H., & Author, C. (n.d.). *Pavement Image Datasets : A New Benchmark Dataset to Classify and Densify Pavement Distresses*.
- Mandal, V., Uong, L., & Adu-gyamfi, Y. (2018). Automated Road Crack Detection Using Deep Convolutional Neural Networks. *2018 IEEE International Conference on Big Data (Big Data)*, May 2019, 5212–5215. <https://doi.org/10.1109/BigData.2018.8622327>
- Mohan, A., & Poobal, S. (2017). Crack detection using image processing : A critical review and analysis. *Alexandria Engineering Journal*. <https://doi.org/10.1016/j.aej.2017.01.020>
- Ouyang, A., Dong, Q., Wang, Y., & Liu, Y. (2014). *The Classification of Pavement*

Crack Image Based on Beamlet Algorithm. 129–137.

- Safaei, N., Smadi, O., Masoud, A., & Safaei, B. (2021). An Automatic Image Processing Algorithm Based on Crack Pixel Density for Pavement Crack Detection and Classification. *International Journal of Pavement Research and Technology*, 0123456789, 16–18. <https://doi.org/10.1007/s42947-021-00006-4>
- Safaei, N., Smadi, O., Masoud, A., & Safaei, B. (2022). An Automatic Image Processing Algorithm Based on Crack Pixel Density for Pavement Crack Detection and Classification. *International Journal of Pavement Research and Technology*, 15(1), 159–172. <https://doi.org/10.1007/s42947-021-00006-4>
- Yang, J., Fu, Q., & Nie, M. (2019). *Deep convolution neural network for crack detection on asphalt pavement* Deep convolution neural network for crack detection on asphalt pavement. <https://doi.org/10.1088/1742-6596/1349/1/012020>
- Ying, L., & Salari, E. (2010). *Beamlet Transform-Based Technique for Pavement Crack Detection and Classification.* 25, 572–580. <https://doi.org/10.1111/j.1467-8667.2010.00674.x>
- Zhang, A., Wang, K. C. P., Fei, Y., Liu, Y., Li, J. Q., & Chen, C. (2017). *Automated Pixel-Level Pavement Crack Detection on 3D Asphalt Surfaces Using a Deep-Learning Network.* 00, 1–15. <https://doi.org/10.1111/mice.12297>
- Zhao, H., & Wang, X. (2010). *Improvement of Canny Algorithm Based on Pavement Edge Detection.* 964–967.
- Deng, L., Zhang, A., Guo, J., & Liu, Y. (2023). An Integrated Method for Road Crack Segmentation and Surface Feature Quantification under Complex Backgrounds. *Engineering*, C. (n.d.). *ROAD CRACK DETECTION USING DEEP CONVOLUTIONAL NEURAL NETWORK* Lei Zhang , Fan Yang , Yimin Daniel Zhang , and Ying Julie Zhu.
- Huang, Z., Chen, W., Al-tabbaa, A., & Brilakis, I. (2022). *NHA12D: A NEW PAVEMENT CRACK DATASET AND A COMPARISON STUDY OF CRACK DETECTION ALGORITHMS.*
- Mei, Q., & Gül, M. (2020). A cost effective solution for pavement crack inspection using cameras and deep neural networks. *Construction and Building Materials*, 256, 119397. <https://doi.org/10.1016/j.conbuildmat.2020.119397>
- Salman, M., Mathavan, S., Kamal, K., & Rahman, M. (2013). *Pavement Crack Detection Using the Gabor Filter.* *Itsc*, 2039–2044.
- Song, W., Jia, G., Jia, D. I., & Zhu, H. (2019). Automatic Pavement Crack Detection and Classification Using Multiscale Feature Attention Network. *IEEE Access*, PP, 1. <https://doi.org/10.1109/ACCESS.2019.2956191>

- Thi, N., Nguyen, H., & Perry, S. (n.d.). *Pavement Crack Detection using Convolutional Neural Network*. 16–21.
<https://doi.org/10.1145/3287921.3287949>
- Tsai, Y., Kaul, V., & Mersereau, R. M. (2010). *Critical Assessment of Pavement Distress Segmentation Methods*. January, 11–19.
- Zalama, E., Jaime, G., & Medina, R. (2014). *Road Crack Detection Using Visual Features Extracted by Gabor Filters*. 29, 342–358.
<https://doi.org/10.1111/mice.12042>

Appendix

Appendix A MATLAB code

```

% Clear memory and command window
clc,clear,close all;
warning off

%% Uploading input image
[filename,pathname] = uigetfile('*.','Choose the
input image');
im = imread([pathname,filename]);
% set the image size to suitable value
scale = 600/(max(size(im(:,:,1))));
im = imresize(im,scale*size(im(:,:,1)));
% % Image resize
[m,n,~] = size(im);

%% Image processing
% Convert image from RGB to gray scale
I = rgb2gray(im);

% Image enhancement
% First) 9*9 low pass filter
[f1,f2]=freqspace(size(I),'meshgrid');
D=100/size(I,1);
LPF = ones(9);
r=f1.^2+f2.^2;
for i=1:9
    for j=1:9
        t=r(i,j)/(D*D);
        LPF(i,j)=exp(-t);
    end
end
% Second) applying filter
Y=fft2(double(I)); Y=fftshift(Y);
Y=convn(Y,LPF); Y=ifftshift(Y);
I_en=ifft2(Y);
% Third) blurr image
I_en=imresize(I_en,size(I));
I_en=uint8(I_en);
I_en=imsubtract(I,I_en);
I_en=imadd(I_en,uint8(mean2(I)*ones(size(I))));

% Segmentation of image
level = roundn(graythresh(I_en),-2); % Calculate
threshold using Otsu's method

```

```

BW = ~im2bw(I_en,level); % Convert image to binary
image using threshold
BW = double(BW);

% Removing noise and connecting image
i = 25; BW1 = BW;
while 1
    BW2 = BW1; i = i + 1;
    BW1 = imdilate(BW1,strel('disk',i)); % dilate
image
    BW1 = bwmorph(BW1,'bridge',inf); %
connecting close parts
    BW1 = imfill(BW1,'holes'); % filling
small spaces
    BW1 = imerode(BW1,strel('disk',i-1)); % erode
image
    tmp = bwareafilt(BW1,1); % get size
of biggest connected shape
    tmp = fix(0.05*sum(sum(tmp))); % size
considered noise
    BW1 = bwareaopen(BW1,tmp); % remove
isolated pixels
    CC = bwconncomp(BW1);
    if CC.NumObjects<2,break;end % break
the loop at convergence
end
B = bwboundaries(BW1); % Cracks boundaries

%% Claculating cracks dimensions
Dist = zeros(length(B),1); % Preallocation
a = Dist; b = Dist; % Preallocation
for i=1:length(B)
    tmp = B{i};
    D = pdist2(tmp,tmp); % Euclidean distance
between each 2 points
    % Value and position of farthest 2 points
    [D,tmp] = max(D); [Dist(i),b(i)] = max(D); a(i)
= tmp(b(i));
end

%% Showing results
figure('Position',[76,84,1249,578])
subplot(2,2,1),imshow(I,[]);
title('Gray scale Image');

```

```

subplot(2,2,2),imshow(I_en, []);
title('Enhancement image');

subplot(2,2,3),imshow(BW, []);
title(['Segmented Image -- Threshold =', num2str(level)]);

subplot(2,2,4),imshow(BW1, []);
title('Removed noise Image');

x = inputdlg('Enter the area of image in M^2:', ...
            'Sample', [1 50]);
A = str2double(x{:});
Dist = Dist*sqrt(A/(n*m)); % convert distances into
meters

figure,imshow(im);hold on
for i=1:length(B)
    tmp = B{i};
    plot(tmp(:,2),tmp(:,1),'r','LineWidth',2);
    plot([tmp(a(i),2),tmp(b(i),2)],[tmp(a(i),1),...
        tmp(b(i),1)], '*-b','LineWidth',2);

    text(1+0.5*sum([tmp(a(i),2),tmp(b(i),2)]),1+0.5*sum(
        [tmp(a(i),1),...

        tmp(b(i),1)]), num2str(Dist(i)), 'Color','k','FontSize
        ',20);
end
hold off,title('Final Result');
warning on

```

Appendix B Ethics Certificate



BİLİMSEL ARAŞTIRMALAR ETİK KURULU

04.09.2023

Dear Hassan Idow Mohammed

Your project **“DEVELOPING AN ASPHALT PAVEMENT CRACK DETECTION AND CLASSIFICATION MODEL BY USING BEAMLET TRANSFORM ALGORITHM ”** has been evaluated. Since only secondary data will be used the project, it does not need to go through the ethics committee. You can start your research on the condition that you will use only secondary data.

Prof. Dr. Aşkın KİRAZ

Rapporteur of the Scientific Research Ethics Committee

Appendix C Turnitin Similarity Report

Hassan Idow Mohammed

INBOX | NOW VIEWING: NEW PAPERS ▾



<input type="checkbox"/>	AUTHOR	TITLE	SIMILARITY	GRADE	RESPONSE	FILE	PAPER ID	DATE
<input type="checkbox"/>	Hassan Idow Mohammed	abstract	0% ■	--	--	📄	2179449438	28-Sep-2023
<input type="checkbox"/>	Hassan Idow Mohammed	Chapter V-Conclusion	0% ■	--	--	📄	2179450939	28-Sep-2023
<input type="checkbox"/>	Hassan Idow Mohammed	Chapter II-Literature Review	2% ■	--	--	📄	2179450263	28-Sep-2023
<input type="checkbox"/>	Hassan Idow Mohammed	Chapter I-Introduction	3% ■	--	--	📄	2179450003	28-Sep-2023
<input type="checkbox"/>	Hassan Idow Mohammed	Chapter III-Methodology	4% ■	--	--	📄	2179450464	28-Sep-2023
<input type="checkbox"/>	Hassan Idow Mohammed	Chapter IV-Result and Discussion	4% ■	--	--	📄	2179450759	28-Sep-2023
<input type="checkbox"/>	Hassan Idow Mohammed	📄 Full Thesis-20227196	13% ■	--	--	📄	2179451411	28-Sep-2023